Doppler-Shift Lifetime Measurements in the p and s-d Shells Using Lithium Reactions*

M. J. THROOP†

Department of Physics and Astronomy, University of Iowa, Iowa City, Iowa 52240

(Received 22 July 1968)

The Doppler-shift-attenuation method was used to deduce lifetime information for electromagnetic transitions in B^{10}, B^{11}, B^{12}, B^{13}, C^{11}, C^{14}, N^{14}, N^{15}, N^{16}, N^{17}, O^{16}, F^{18}, Ne^{20}, and Ne^{21}. The combination of a Ge(Li) γ-ray detector and the use of lithium reactions permitted an accurate measurement of numerous lifetimes as well as the setting of improved limits for very fast lifetimes. In addition, a number of transition energies were measured with improved accuracy.

I. INTRODUCTION

THE relatively large recoil velocities characteristic of residual nuclei produced in heavy-ion reactions have long been recognized as an important advantage in the measurement of nuclear lifetimes by the Doppler-shift-attenuation method.[1] The analysis of Doppler-shifted lines in lithium-induced reaction spectra obtained with NaI(Tl) detectors was seriously limited in the past by resolution and source identification difficulties for the numerous lines observed.[2] The much-improved resolution obtained using Ge(Li) detectors has essentially removed these difficulties.

The lifetime information which can be obtained from a study of γ-ray singles spectra is, of course, limited to the case of residual nuclei kinematically restricted to stopping in the target and backing materials. In addition, a lifetime determination for a level populated by γ-ray cascade necessarily requires that the lifetimes of the populating levels be known. Subject to these limitations, singles spectra can still yield a considerable amount of lifetime information.

The results reported in the following sections are for nuclei produced in Li^6 and Li^7 reactions with isotopes of Li, Be, B, C, and O. The results are largely limited to transitions in p-shell nuclei. Spectra containing transitions from s-d-shell nuclei were generally too complicated to study without recourse to coincidence techniques. Transitions in N^{17} were deemed of sufficient interest to be investigated using rather limited proton-γ coincidence studies in the $B^{11}(Li^7, p)N^{17}$ reaction.

The relatively large recoil velocities obtained for these lithium-induced reaction products [$\beta = v/c \sim (1.5\text{–}2.3) \times 10^{-2}$] ensured that decays occurred primarily in the velocity region for which electronic stopping predominated. Effects due to nuclear stopping and scattering were thus expected to have a relatively small influence on the deduced lifetime results.

II. EXPERIMENTAL PROCEDURE

Singly charged Li^6 and Li^7 ions of energy ranging from 5.1 to 6.3 MeV were obtained from the University of Iowa 5.5-MeV Van de Graaff accelerator. The ion source and operating parameters have been described elsewhere.[3] After momentum analysis and deflection by a switching magnet, the Li beam was brought to a focus at the entrance to a collimating system located 29 ft from the switching magnet.

The first element of the collimating system was a 6-mm-diam canal in a 2-in.-diam by 2.25-in.-long aluminum plug. This canal served the double purpose of beam definition and isolation of the target-chamber vacuum system. The target-chamber vacuum system pumping elements consisted of an in-line 20-liter-sec titanium-ion pump and a liquid-nitrogen cold trap located in the bottom of the target chamber. The chamber vacuum system was designed for minimal hydrocarbon contamination. It was found that although carbon and oxygen were present as original target contaminants and some additional buildup of these contaminants did occur, the level of contamination was in all cases small enough to contribute negligibly to the γ-ray spectra. The beam was further defined by a 3-mm-diam tantalum aperture separated by a 4-in. lead spacer from an antiscattering aperture. This assembly was located 48 in. from the 6-mm canal and 42 in. from the target chamber. The lead spacer was designed to shield the Ge(Li) detector from γ rays generated at the 3-mm aperture. The lead spacer combined with the remote location of the apertures reduced aperture γ-ray background to unobservably small proportions. The collimation system restricted the angular divergence of the beam to a cone with a half-angle of 0.2°. The beam-spot diameter on the target was 5 mm or less, depending on focusing conditions.

The target chamber was a cylinder of 6.5-in. inside diameter with a wall thickness of 0.125 in. and a height of 7.25 in. The chamber top and body were constructed of aluminum; the bottom plate containing the cold-trap assembly was of stainless steel. The cylindrical

* Research supported in part by the National Science Foundation.

† Part of this work was performed while a National Science Foundation Cooperative Graduate Fellow, 1964–1966.

[1] A. E. Litherland, M. J. L. Yates, B. M. Hinds, and D. Eccleshall, Nucl. Phys. **44**, 220 (1963).

[2] R. M. Bahnsen, M.S. thesis, University of Iowa, 1962 (unpublished).

[3] D. W. Heikkinen, Ph.D. thesis, University of Iowa Report No. 65-24, 1965 (unpublished); Phys. Rev. **141**, 1007 (1966).

TABLE I. Table of targets.

Target		Backing	(mg/cm²)	Thickness at 45° (μg/cm²)	Thickness at 45° to 5.5-MeV Li^6 (keV)
Li^6F	(99.3% Li^6)	Al	20.2	156	275
Li^7F	(99.99% Li^7)	Al	20.2	156	275
		Cu	45	156	275
Be	(natural)	Al	8.8	50	108
		Cu	45	200	430
B^{10}	(92.15% B^{10})	Cu	45	86	219
B^{11}	(98.05% B^{11})	Cu	45	86	200
C^{12}	(natural)	Cu	45	40	87
		Al	20.2	62	136
		Al	10	33	73
C^{12}	(~40%)	Ni	0.45	120	243
$+C^{13}$	(~60%)	+Cu	112		
SiO	(natural)	Al	20.2	312	150

symmetry of the chamber ensured that γ-ray absorption effects were the same at all angles of observation.

The 20-cm³ active volume Ge(Li) detector[4] and its Dewar were clamped on a base plate which slid on rails attached to a rotating trolley assembly. The pivot of the trolley assembly was located at the center of a 5-ft-square table inscribed with 15°-interval markings. A ceiling bracket supported the beam line at a point just behind the target-chamber inlet neck. Such a supporting arrangement made it possible to adjust the table position with respect to the chamber without disturbing the alignment of the chamber and aperture system.

The design of the detector mount system permitted the detector angle with respect to the beam direction to be varied from 0° to 150° on either side of the beam axis. The radial distance from the target to the front face of the detector was variable from 8.8 to 15.9 cm. The axis about which the Ge(Li) detector rotated was made to coincide with the center of the target chamber by moving the detector to the 8.8-cm position where the detector housing touched the cylindrical chamber wall. The table position was then adjusted until the detector housing just touched the chamber wall at all angles of rotation of the detector trolley. Using this method of alignment, it is estimated that the distance from the detector to the beam spot could not vary by more than 3 mm, where most of this variation was due to possible movement of the beam spot with varying focusing conditions.

The angle markings on the table were aligned with respect to the beam axis by requiring that the center of the detector housing coincide with the corresponding angle markings inscribed on the chamber itself. The estimated error in angular positioning with respect to the beam direction was ±2.5°. Included in this error estimate is an estimate of the possible noncoincidence of the Ge(Li) detector axis and the axis of the detector housing. The results of a scan of the Ge(Li) detector with a Co^{57} γ-ray source collimated to a 2-mm beam diam indicated that the active volume of the detector was symmetrically distributed about a point within 2 mm of the detector housing axis.

The detector-target distance at which all the data were taken was 15.9 cm. For this distance, the angular attenuation coefficient due to the finite detector solid angle was estimated to be not less than 0.996. The resulting attenuation of the Doppler shift was thus sufficiently small in comparison with other sources of error to be ignored. The error due to a possible angular misalignment of ±2.5° was ±1.1% for a 0°-to-150° shift measurement and ±4.5% for a 0°-to-90° shift measurement. For a 30°-to-150° shift measurement symmetric about 90°), the error due to possible angular misalignment was zero in first order.

The target and backing materials, as well as target thicknesses used, are listed in Table I. The targets were prepared by methods which have previously been described.[3,5–8] The LiF and boron target thicknesses in μg/cm² were calculated from measurements of the evaporation apparatus geometry and weighings of the material to be evaporated. The beryllium, carbon, and SiO target thicknesses were measured by observing the shift of either the $Al^{27}(p, \gamma)Si^{28}$ 991-keV resonance for aluminum-backed targets or the $Cu^{65}(p, n)Zn^{65}$ 2165-keV threshold for copper-backed targets. The proton-stopping-power data of Whaling[9] were then used to calculate the target thicknesses in μg/cm². The final column of Table I lists the target thicknesses in keV to a 5.5-MeV Li^6 beam, where the energy loss to the Li^6 beam was calculated from extrapolated stopping-power data of Allison *et al.*[10] and of Northcliffe.[11] These are typical energy-loss values; the actual values differed from these slightly, depending on the bombarding energy and type of beam. The accuracy of the target-thickness measurements is estimated to be ±25%. In all runs the target was oriented at 45° with respect to the beam such that the Ge(Li) detector viewed the front face of the target when placed at 90° with respect to the beam axis.

[4] Princeton Gamma Tech, Inc., Princeton, N.J.

[5] K. G. Kibler, Ph.D. thesis, University of Iowa Report No. 66-30, 1966 (unpublished); Phys. Rev. **152**, 932 (1966).

[6] W. A. Seale, Ph.D. thesis, University of Iowa Report No. 67-3, 1967 (unpublished); Phys. Rev. **160**, 809 (1967).

[7] V. P. Hart, Ph.D. thesis, University of Iowa Report No. 64-26, 1964 (unpublished).

[8] R. B. Parsons, M.S. thesis, University of Iowa Report No. 66-35, 1966 (unpublished).

[9] W. Whaling, in *Handbuch der Physik*, edited by S. Flügge (Springer-Verlag, Berlin, 1958), Vol. XXXIV, p. 193.

[10] S. K. Allison, D. Auton, and R. A. Morrison, Phys. Rev. **138**, A688 (1965).

[11] L. C. Northcliffe, Ann. Rev. Nucl. Sci. **13**, 67 (1963).

For purposes of spectral analysis and source identification, the γ-ray energy-dependent response of the Ge(Li) detector was parametrized in terms of the two-escape to full-energy peak ratio, the two-escape to one-escape peak ratio, and the absolute detector efficiency, for a 15.9-cm source-detector distance. The escape-peak-ratio determinations were based on measurements with routinely available γ-ray sources as well as for spectra containing intense lines with clearly identifiable escape and full-energy components. The detector-efficiency curve was constructed from a set of relative efficiencies for pairs of γ-ray lines, where the relative intensities of the lines were well known. Such pairs spanned the energy range 280 keV–8.6 MeV, and included those from sources such as Na^{22}, Na^{24}, and Co^{60},[12] as well as those from reaction-produced residual nuclei for which branching ratios have been determined with some accuracy, such as B^{11}, N^{14}, and N^{16}.[13–15]

The electronics system consisted of the Ge(Li) detector, a low-noise FET preamplifier and main amplifier with variable time constants,[16] and a 4096-channel analog-to-digital converter (ADC).[17] The amplifier time constants were selected for optimum γ-ray resolution, which ranged from 5.5-keV full width at half-maximum (FWHM) for a 1.33-MeV full-energy peak to 9.5-keV FWHM for a 5.1-MeV two-escape peak. For the amplifier time constants used, the counting rate was kept to 2000 cps or less to prevent loss of resolution due to pileup effects.

For runs of longer than 2-h duration it was found necessary to stabilize the gain of the electronics system. This was accomplished by injecting the output from a high-stability pulser[18] into the preamplifier input section. The resulting pulser peak, set at the high-energy end of the pulse-height spectrum, was the reference line for a digital stabilizer[17] which supplied gain correction signals to the ADC. The gain stability of the resulting system was found to be ± 1 channel in 3700 in a 24-h period. The system was not stabilized against zero-level drift but the presence of intense low-energy lines such as 511-keV annihilation radiation made it possible to monitor and correct for such a drift.

A limited particle-γ coincidence study was carried out for the $B^{11}(Li^7, p)N^{17}$ reaction. The particle detector was a lithium-drifted silicon detector with an active area of 500 mm^2 and a depletion depth of 3 mm.[19] The detector was mounted on a clamp connected to the cold-trap assembly and was operated at liquid-nitrogen temperatures. The particle detector was located at 140° and subtended 45° in the lab, so that individual proton groups corresponding to levels in N^{17} could not be resolved. The Q values for charged particles from the $B^{11}(Li^7, p)$ reaction were such that a 20-mg/cm^2 Al foil in front of the particle detector stopped all excited-state charged-particle groups except protons. The accumulated coincidence spectrum was therefore a spectrum of γ-ray transitions resulting from the population of many N^{17} states. Standard fast-slow coincidence electronics were used to generate an ADC gate signal whenever a fast ($2\tau \sim 100$ nsec) coincidence occurred between events above discriminator levels in both the γ and particle detectors.

During data acquisition, pulses were digitized by the ADC and stored in the 8190-word memory of a digital computer. The computer was programmed for the storage of a 3967-channel pulse-height spectrum in the double-precision mode, so that up to $\sim 16 \times 10^6$ counts per channel could be accumulated before overflow occurred.

III. DATA REDUCTION

A. Source Identification and Background Subtaction

A preliminary energy calibration was made using calibration points from ThC″ and Co^{60} spectra taken at intervals between groups of runs. Additional calibration points included those for several lines of well-known energy in the spectra under study. A least-squares fit using a polynomial of the form

$$E_\gamma = \sum_{i=0}^{N} A_i x^i,$$

where x is the channel number, and N was varied from 1 to 4, was performed for such calibration points. Such a fit was found to be accurate to ± 7 keV over most of the usable range of analyzer channels. This accuracy was sufficient for the identification of the sources of most observed lines. The sources considered included possible transitions in the residual nuclei produced in the reaction under study and also in lithium-oxygen and lithium-carbon target contaminant reactions. The lithium-oxygen and lithium-carbon reactions were themselves investigated, so that the lines from these contaminant reactions were known in both energy and relative intensity. Other sources considered included levels in germanium and aluminum which were excited by reaction neutrons inelastically scattered from the Ge(Li) detector and nearby aluminum.[20] No neutron-induced lines were observed above 2.2 MeV. In addition, it was found necessary to consider lines due to lithium reactions with the aluminum target backing

[12] W. R. Kane and M. A. Mariscotti, Nucl. Instr. Methods **56**, 189 (1967).
[13] J. W. Olness, E. K. Warburton, D. E. Alburger, and J. A. Becker, Phys. Rev. **139**, B512 (1965).
[14] S. Gorodetzky, R. M. Freeman, A. Gallmann, and F. Haas, Phys. Rev. **149**, 801 (1966).
[15] J. M. Freeman and R. C. Hanna, Nucl. Phys. **4**, 599 (1957).
[16] Tennelec, Inc., Oak Ridge, Tenn.
[17] Nuclear Data, Inc., Palatine, Ill.
[18] Berkeley Nucleonics Co., Berkeley, Calif.
[19] Simtec, Ltd., Montreal, Quebec.
[20] C. Chasman, K. W. Jones, and R. A. Ristinen, Nucl. Instr. Methods **37**, 1 (1965).

used in some runs and with the fluorine in LiF targets. Finally, long-lived β emitters left over from previous runs were considered as possible sources; prominent among these was Na^{24} formed in the reaction $F^{19}(Li^7, d)Na^{24}$ with a 15-h half-life.

The determination of possible sources for observed lines was based on recent compilations of level energies, branching ratios, and lifetime information for $Z=2$–10 [21–23] and $Z=10$–20.[24]

Doppler-shift and -broadening analysis required the subtraction of background underneath peaks of interest and determination of peak centroids. The background subtraction was performed by generating a least-squares fit to selected portions of the background spectrum on either side of a particular peak. In this method, the background underneath a peak was assumed to be accurately represented by a smooth extension of the background on either side of a peak. It was found that most types of background encountered could be adequately fitted by a polynomial of the form

$$Y_i = \sum_{j=0}^{N} A_j (x_i)^j,$$

where Y_i is the fitted number of counts in channel i, x_i is the channel number of the ith channel, and the A_j's are the coefficients of the fit. The polynomial order N was increased until an acceptable χ^2 was obtained. A value of N greater than 2 or 3 was usually not necessary except for fits to rapidly varying background, such as that near a Compton edge. It was found that acceptable background fits could be obtained as long as the region to be fitted was confined to a reasonably small region on either side of the peak of interest.

An estimate of the possible error in the location of the peak centroids was made by varying the extent and location of the region used in the background fit. It was found that in most cases the variation of the peak centroid with choice of background region was $\lesssim 0.3$ channel for well-localized peaks. The possible error was larger for cases in which the background was not smoothly varying in the region of interest (for example, near a Compton edge).

An incidental result of the present work was an accurate determination of a number of γ-ray transition energies. A determination of such transition energies was undertaken only for those cases in which the accuracy was a significant improvement over that of previously reported determinations. The method of energy calibration for the spectra was similar to that described previously for the preliminary calibration. The energies of lines of interest were determined from the 90° (unshifted) spectrum, using other lines of well-known energy in the same spectrum as calibration points.[25] This method of internal calibration was a necessity for high-energy transition measurements, since no natural sources of high-energy γ rays were available. Further, the use of internal calibration points avoided the problems associated with gain and zero shifts which could occur between the accumulation of calibration and reaction spectra. Since the high-energy transition determinations employed nearby lines as calibration points, any error contributed by system nonlinearities was minimized. The estimated error due to system nonlinearities was generally small compared to other sources of error such as that due to uncertainty in the peak-centroid location.

A significant source of error in the energy of Doppler-broadened lines detected at 90° to the beam axis was that due to possible angular misalignment of the detector. This error was $\pm 4.5\%$ of the 0°-to-90° shift, or in some cases as much as ± 7 keV. The weighted average from a sufficient number of determinations was not expected to be seriously affected by this random source of error. Results based on only one or two measurements were assigned appropriately large errors.

The energy of a Doppler-broadened line measured at 90° to the beam axis equals the transition energy only if terms to second order in β can be neglected in the Doppler-shift relation.[26] For the largest values of β encountered in this work, the expected difference between the 90° energy and the transition energy was less than 2 keV. This was not significant compared to other sources of error.

B. Doppler-Shift-Attenuation Method

The average γ-ray energy emitted from nuclei m_4^* produced in the reaction $m_1+m_2 \rightarrow m_3+m_4^*+Q$ is, to first order in $\beta=v/c$,

$$\langle E_\gamma \rangle = E_{\gamma_0}[1+F(\tau)\,\langle \beta(0) \rangle \cos\theta_\gamma], \qquad (1)$$

where E_{γ_0} is the γ-ray energy for m_4^* decaying at rest,

[21] *Nuclear Data Sheets*, compiled by K. Way *et al.* (Printing and Publishing Office, National Academy of Sciences–National Research Council, Washington, D.C. 20025), NRC 60-1-22.

[22] F. Ajzenberg-Selove and T. Lauritsen, Nucl. Phys. **11**, 1 (1959).

[23] T. Lauritsen and F. Ajzenberg-Selove, Nucl. Phys. **78**, 1 (1966).

[24] P. M. Endt and C. Van der Leun, Nucl. Phys. **34**, 1 (1962).

[25] Calibration energies were based on a variety of published results. Of particular value were energies from the following compilation: J. B. Marion, Nucl. Data **4**, 301 (1968). Also used were recent Ge(Li) results for N^{14}: D. E. Alburger, A. Gallmann, J. B. Nelson, J. T. Sample, and E. K. Warburton, Phys. Rev. **148**, 1050 (1966); N^{15}: E. K. Warburton, J. W. Olness, and D. E. Alburger, *ibid.* **140**, B1202 (1965); and Ne^{20}: D. E. Alburger and K. W. Jones, *ibid.* **149**, 743 (1966). In addition, the magnetic-spectrometer results of the Notre Dame group were used for B^{11}: C. P. Browne and F. H. O'Donnell, *ibid.* **149**, 767 (1966); and O^{16}: C. P. Browne and I. Michael, *ibid.* **134**, B133 (1964).

[26] T. K. Alexander, A. E. Litherland, and C. Broude, Can. J. Phys. **43**, 2310 (1965).

$\langle\beta(0)\rangle$ is the average component of the initial ($t=0$) m_4* recoil velocity projected along the m_1 beam axis, θ_γ is the angle of observation of γ radiation with respect to the beam axis, and $F(\tau)$ is the Doppler-shift-attenuation factor.[27] $\langle\beta(0)\rangle$ may be evaluated from

$$\langle\beta(0)\rangle=\langle\beta_{\text{c.m.}}(0)+\beta_r(0)\cos\theta_{\text{c.m.}}\rangle$$
$$=\beta_{\text{c.m.}}[1+R\langle\cos\theta_{\text{c.m.}}\rangle], \quad (2)$$

with

$$R=\frac{\beta_r}{\beta_{\text{c.m.}}}=\left[\frac{m_2m_3}{m_1m_4}\left(1+\frac{m_1+m_2}{m_2}\frac{Q}{E_B}\right)\right]^{1/2}, \quad (3)$$

where $\beta_{\text{c.m.}}$ is the lab velocity of the c.m. system, β_r is the m_4* recoil velocity in the c.m. system, and E_B is the incident m_1 lab energy. Note that for $R<1$, the maximum m_4* recoil angle is just $\sin^{-1}R$. The average projected m_4* c.m. angle is

$$\langle\cos\theta_{\text{c.m.}}\rangle=\left(\int\sigma(\theta_{\text{c.m.}})W(\theta_{\text{c.m.}},\phi,\theta_\gamma)\cos\theta_{\text{c.m.}}\sin\theta_{\text{c.m.}}d\Omega_{\text{c.m.}}\right)\Big/\int\sigma(\theta_{\text{c.m.}})W(\theta_{\text{c.m.}},\phi,\theta_\gamma)\sin\theta_{\text{c.m.}}d\Omega_{\text{c.m.}}, \quad (4)$$

where $\sigma(\theta_{\text{c.m.}})$ and $W(\theta_{\text{c.m.}},\phi,\theta_\gamma)$ are the m_4* c.m. angular distribution and angular correlation functions.

The Doppler-shift-attenuation factor was determined experimentally through a measurement of $\langle E_\gamma\rangle$ at two angles with respect to the beam axis, $\theta_{\gamma1}$ and $\theta_{\gamma2}$ [28]:

$$F'=\frac{\langle E_{\gamma1}\rangle-\langle E_{\gamma2}\rangle}{\beta_{\text{c.m.}}(1+R\langle\cos\theta_{\text{c.m.}}\rangle)(\cos\theta_{\gamma1}-\cos\theta_{\gamma2})}. \quad (5)$$

The mean lifetime of the γ-decaying state was that τ for which $F(\tau)$ equaled the experimentally determined F', where

$$F(t)=\langle\bar\beta\rangle/\langle\beta(0)\rangle$$
$$=[\tau\langle\nu(0)\rangle]^{-1}\left\langle\int_0^\infty\exp(-t/\tau)\nu(t)\langle\cos\Phi(\nu)\rangle dt\right\rangle. \quad (6)$$

$\bar\beta$ is the average velocity at which m_4* decay occurs and ν is a convenient dimensionless velocity parameter defined as v/v_0, where $v_0=c/137$. The brackets refer to an average over the kinematically allowed distribution of m_4* lab. ν's projected on the beam axis and weighted by $\sigma(\theta_{\text{c.m.}})W(\theta_{\text{c.m.}},\phi,\theta_\gamma)\sin\theta_{\text{c.m.}}$. The $\langle\cos\Phi(\nu)\rangle$ term is the average nuclear scattering projection factor as determined from the formalism of Blaugrund.[29]

The function $\nu(t)$ was determined from integration of the relation

$$dE/dX=m_4v_0(d\nu/dt), \quad (7)$$

where dE/dX is the stopping power of the target or backing material for the ion of mass m_4.

The line shape is determined in part by the distribution of shifts

$$dN(t)/d\nu=\frac{dN/dt}{d\nu/dt}$$
$$=(m_4v_0/\tau)\exp(-t/\tau)[dE(\nu)/dX]^{-1}, \quad (8)$$

with $N=N_0\exp(-t/\tau)$ ($N_0\equiv1$), where $dN(t)/d\nu$ is the distribution of decays over the range $\nu(0)$ to $\nu(t)=0$. For each element $d\nu$ of the above distribution, the velocity vector $\nu(t)\langle\cos\Phi(\nu)\rangle$ has a distribution of kinematically allowed directions in space. Thus an additional distribution of γ-ray energies arises from the projections of $\nu(t)\langle\cos\Phi(\nu)\rangle$ along the direction of observation θ_γ, weighted by the angular correlation function W. The sum of such distributions, each corresponding to an initial velocity $\nu(0)$ and weighted by the angular distribution function σ, constitutes the line shape for a particular τ.

The maximum kinematically allowed line broadening ΔE_γ is, from Eqs. (1) and (2),

$$\Delta E_\gamma=2\beta_rE_{\gamma0}. \quad (9)$$

An estimate for the lifetime of a state can be made by comparing the maximum kinematically allowed broadening with the observed linewidth (for example, the FWHM). Since the observed linewidth is also modulated by the angular distribution and angular correlation functions, the deduced lifetime is in the nature of an upper limit.

The stopping-power data necessary for the evaluation of $F(\tau)$ and the determination of line shapes were obtained largely from the electronic-stopping-power

[27] Equation (1) and those following are derived on the assumption of an azimuthally symmetric distribution of m_4* nuclei. Then the average projected m_4* velocity vector $\langle\beta(0)\rangle$ is directed along the beam axis. The derivation is also based on a second assumption, namely, an azimuthal symmetry of the target and backing stopping media about $\langle\beta(0)\rangle$. Then $\langle\beta(0)\rangle$ and $\langle\bar\beta\rangle$, the average velocity at which decay occurs, are collinear. The two assumptions taken together require that the target material in which the nuclei stop be the same for all azimuthal directions, a condition not always met in the present work. An estimate of the error introduced by a distribution of stopping media not symmetric about $\langle\beta(0)\rangle$ is discussed in Sec. III D.

[28] The denominator of Eq. (5) should be written

$$\beta_{\text{c.m.}}[(1+R\langle\cos\theta_{\text{c.m.}}\rangle_1)\cos\theta_{\gamma1}-(1+R\langle\cos\theta_{\text{c.m.}}\rangle_2)\cos\theta_{\gamma2}],$$

where the subscripts 1 and 2 on $\langle\cos\theta_{\text{c.m.}}\rangle$ refer to evaluation of W at $\theta_{\gamma1}$ and $\theta_{\gamma2}$. See, for example, P. Paul, J. B. Thomas, and S. S. Hanna, Phys. Rev. **147**, 774 (1966). Since W and σ were generally not known for the reactions studied in this work, the uncertainty in $\langle\beta(0)\rangle$ was collected in the $\langle\cos\theta_{\text{c.m.}}\rangle$ term as written in Eq. (5). Equation (5) is, of course, correct for an angular correlation function W isotropic in θ_γ.

[29] A. E. Blaugrund, Nucl. Phys. **88**, 501 (1966).

results of Porat and Ramavataram,[30] which span the velocity range and variety of stopping materials for the nuclei studied in this work. In the case of B and F ions stopping in various materials, it was necessary to extrapolate from data for ions of nearby atomic number, such as C and Ne. The extrapolation procedure followed for the electronic stopping power was that described by Northcliffe.[11] Since the data of Porat and Ramavataram did not extend below $v=1$, these data were linearly extrapolated to $v=0$ in accordance with the predicted linear dependence of dE/dX on v for $v\leq Z^{2/3}$, where Z is the atomic number of the m_4 ion.[31] Where comparison of the extrapolated data for $v\leq 1$ was possible, good agreement was obtained with the results of Ormrod and collaborators.[32] The nuclear stopping power was calculated using the analytical expressions of Blaugrund[29] and of Baker[33] based on the theory of Lindhard *et al.*[31]

In general, very little information was available regarding either the angular distribution or angular correlation functions for reactions producing the nuclear states studied in this work. It was therefore necessary to determine a set of limits within which $\langle\cos\theta_{\text{c.m.}}\rangle$ could be expected to fall. Assuming an isotropic angular correlation function, $\langle\cos\theta_{\text{c.m.}}\rangle$ was evaluated for 35 charged-particle angular distributions from the Li^6+Li^7, Li^7+Be^9, and Li^6+C^{12} reactions.[3,34,35] The average value of $\langle\cos\theta_{\text{c.m.}}\rangle$ is 0, and in all cases falls within the limits ± 0.25. Under the reasonable assumption that σ and W are similar in character and uncorrelated, the value for $\langle\cos\theta_{\text{c.m.}}\rangle$ becomes 0.0 ± 0.35. Note that the limits are essentially two-standard-deviation limits. For reactions involving identical incoming nuclei, such as Li^6+Li^6 and Li^7+Li^7, $\langle\cos\theta_{\text{c.m.}}\rangle$ is, of course, identically zero.

The calculations necessary for the determination of $F(\tau)$ and the line shape were performed by a computer code written for the purpose. The input consisted of the electronic-stopping-power data for the m_4 ion stopping in the appropriate target and backing materials, as well as angular-distribution data when available. The essential function performed by the computer code was the detailed averaging necessary for the rather extensive velocity distributions kinematically allowed for the reactions under study.

Not all peaks observed in the spectra could be unambiguously analyzed for a lifetime or lifetime limit. A peak was considered suitable for analysis if the following requirements were met:

(a) The reaction kinematics were such that $R=\beta_r/\beta_{\text{c.m.}}<0.707$. This requirement ensured recoil of the decaying nucleus into the target and backing material for the usual case of the target normal inclined at 45° with respect to the beam axis.

(b) No feeding of the state of interest via γ-ray cascades from higher-bound excited states unless such states were known to have lifetimes much shorter or much longer than the state of interest. An estimate of the extent of cascade feeding from higher states as well as their approximate lifetimes could be made by examining the magnitude and shift of the cascade peaks in the spectrum under study.

(c) No contamination of the line of interest by other transitions of nearly the same energy. The presence of such contamination was checked for by examining the $\theta_\gamma=90°$ peak for nonsymmetrical shape. In addition, a tabulation was made of all possible transitions in the residual nuclei produced in all the reactions studied. This tabulation was always examined for a possible energy coincidence between the transition of interest and some other possible transition.

The following sections contain examples of the analysis of data for the first excited state of B^{12}, for several excited states of B^{11}, and for the first excited state of Ne^{20}. These examples substantially cover the range of lifetimes encountered in this work.

C. Lifetime of the B^{12} First Excited State

The decay of the B^{12} 953-keV first excited state was observed in the Li^7+Li^7 γ-ray spectrum (Fig. 1). Spectra were observed for an aluminum-backed 110-$\mu g/cm^2$ Li^7F target at γ-ray angles of 0°, 90°, and 150° with respect to the beam axis, at an incident energy of 5.42 MeV.

In order to determine the distribution of initial B^{12} velocities, it is necessary to consider the possible ways in which the $B^{12}(953)$ state may be formed. The important modes of formation are

(1) $Li^7+Li^7\rightarrow B^{12}(953)+d$, $Q=2.353$ MeV

(2) $\rightarrow B^{12}(953)+p+n$, $Q=0.129$ MeV

(3) $\rightarrow B^{12}(2621)+d$, $Q=0.685$ MeV

(4) $\rightarrow B^{12}(2621)+p+n$, $Q=-1.539$ MeV.

Reactions 3 and 4 lead to the population of the 953-keV state through a 2621→953-keV 80% branch[36] (see the B^{12} decay scheme in Fig. 1). Population of the 2621-keV level through reactions 3 and 4 also leads to a 948-keV line due to a 2621→1674-keV 14% branch, which, if

[30] D. I. Porat and K. Ramavataram, Proc. Roy. Soc. (London) **A252**, 394 (1959); Proc. Phys. Soc. (London) **77**, 97 (1961); **78**, 1135 (1961).

[31] J. Lindhard, M. Scharff, and H. E. Schiøtt, Kgl. Danske Videnskab. Selskab, Mat.-Fys. Medd. **33**, No. 14 (1963).

[32] J. H. Ormrod and H. E. Duckworth, Can. J. Phys. **41**, 1424 (1963); J. H. Ormrod, J. R. MacDonald, and H. E. Duckworth, *ibid.* **43**, 275 (1964); J. R. MacDonald, J. H. Ormrod, and H. E. Duckworth, Z. Naturforsch. **21**, 130 (1966).

[33] S. I. Baker, Ph.D. thesis, Illinois Institute of Technology, 1967 (unpublished).

[34] K. G. Kibler, Phys. Rev. **155**, 1110 (1967).

[35] R. R. Carlson (private communication).

[36] J. W. Olness and E. K. Warburton, Phys. Rev. **166**, 1004 (1968).

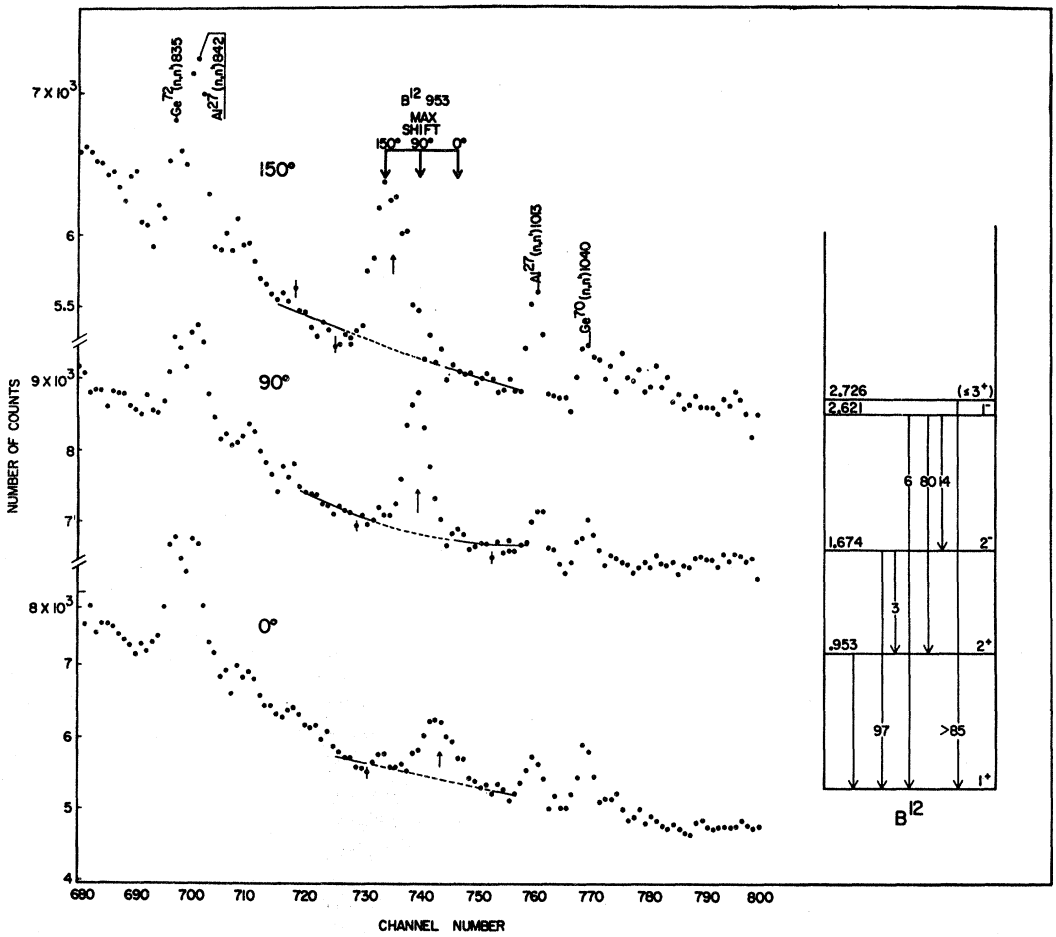

FIG. 1. Portion of the Li^7+Li^7 spectrum, showing the B^{12} 953-keV line as a function of θ_γ. The B^{12} decay scheme is from Ref. 36. The solid curves on either side of the B^{12} 953-keV peak are the best fit to the background region. The dashed line under the peak represents the background interpolated from the fit on either side of the peak. The arrows underneath each peak indicate the location of the peak centroid.

present, could not be easily separated from the 953-keV line of interest.

Charged-particle angular-distribution results have been reported for the Li^7+Li^7 reaction at incident Li^7 energies near those of the present work.[37] The relative contributions of the above four reactions to the population of the $B^{12}(953)$ level were deduced from the angular-distribution data combined with the efficiency-corrected observed intensities of expected lines in the Li^7+Li^7 spectrum. Expressed in percentages, these contributions were determined to be: reaction 1 (35 ± 10), reaction 2 (42 ± 10), reaction 3 (20 ± 10), and reaction 4 (<6). In addition, the 948-keV line from decay of the B^{12} 2621-keV state contaminated the 953-keV line to a negligible extent ($\sim3\%$).

The value of $\langle\cos\theta_{c.m.}\rangle$, necessary for a determination of F', is zero for the Li^7+Li^7 reaction (identical incoming particles). Thus, no knowledge of the angular distribution for reactions 1–3 is required in determining F'. The detailed distribution of initial velocities will, of course, be expected to influence the value of $F(\tau)$. In the approximation of a linear stopping-power curve, $F(\tau)$ does not depend on the initial m_4* velocity. The range of initial velocities for reaction 1 and the stopping-power curves used for B^{12} stopping in the target and backing materials are shown in Fig. 2. The stopping-power curve is not far from linear over most of the range of initial velocities (note that reaction 1 has the greatest variation in initial velocities), and for the lifetime being measured ($\sim3\times10^{-13}$ sec) most decays occur before the nonlinear nuclear stopping and scattering region is reached.

A quantitative estimate of the variation of $F(\tau)$ over the range of B^{12} initial velocities was obtained by comparing the $F(\tau)$'s for each of three reactions contributing to the population of the $B^{12}(953)$ state. The varia-

[37] H. W. Wyborny, University of Iowa Report No. 67-44, 1967 (unpublished).

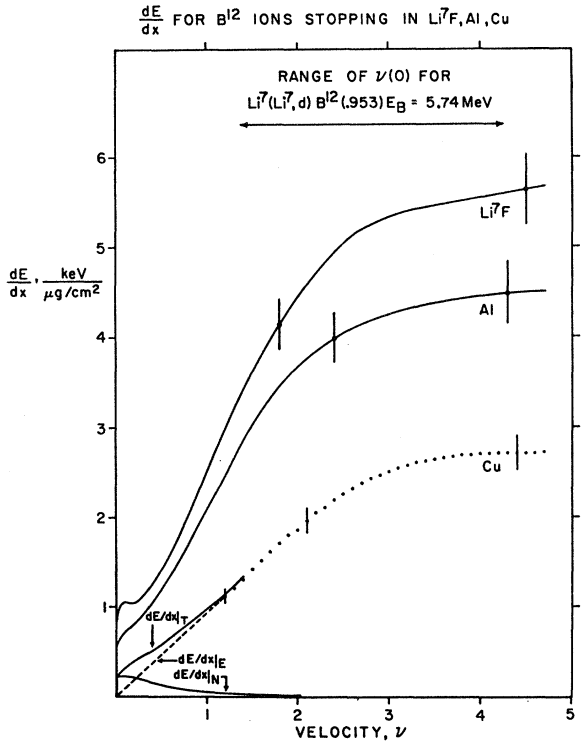

FIG. 2. Stopping power versus v for B^{12} ions stopping in LiF, Cu, and Al. The curve for B^{12} in Cu shows the electronic stopping power $dE/dx|_E$, the nuclear stopping power $dE/dx|_N$, and the total stopping power $dE/dx|_T$.

tion in $F(\tau)$ among reactions 1–3 listed above, for a lifetime of 3×10^{-13} sec, is $\pm1\%$ (assuming reaction 2 to be isotropic or nearly so). It is clear then that $\pm10\%$ error quoted above for the relative reaction amplitudes will lead to a completely negligible error ($<\pm1\%$) in $F(\tau)$.

The observed centroid shift (0°–150°) of the 953-keV line was found to be 8.50 ± 0.30 channels, after a zero-shift correction of 0.1 ± 0.2 channels was made. The zero shift was determined from a measurement of the 0°–150° centroid shift of the 511-keV annihilation and Ne^{21} 351-keV contaminant lines. A check on the shift measurement and background subtraction under the peak was made by comparing the 0°–90° and 90°–150° shifts. The ratio of the 90°–150° to the 0°–90° centroid shift is expected to be 0.866 for the Li^7+Li^7 reaction. The measured centroid-shift ratio was found to be in excellent agreement with the expected value.

The shift in keV was determined using the dispersion (keV/channel) in the 953-keV region obtained from calibration lines in the Li^7+Li^7 spectrum plus lines in Co^{60} and ThC'' spectra accumulated immediately after the last Li^7+Li^7 spectrum. The resulting value of F', and the comparison with $F(\tau)$ to obtain a lifetime, is shown in Fig. 3. The value obtained for the mean lifetime of the B^{12} 953-keV first excited state was

$$\tau_m=(2.95\pm0.37)\times10^{-13}\text{ sec.}$$

There are two major contributions to the error in the result. The first is from the centroid-shift measurement error of $\pm3\%$, which propagates to an error of $\pm10\%$ in τ_m, as shown in Fig. 3. The second source is the error in the stopping-power data used. Since most B^{12} decays occur while stopping in the backing and in the range of v for which electronic stopping predominates (Fig. 2), the major error is that for the electronic stopping power of B ions stopping in Al. The B in Al stopping-power data were generated by conversion from data for C ions stopping in Al, which has a quoted error of $\pm5\%$.[30] The estimated error of the conversion procedure is also $\pm5\%$. These error estimates appear to be reasonable, since an extrapolation to low values of v of the B stopping in Al data generated by conversion is in good agreement with data for B ions of velocity $v=0.1$–0.3 stopping in Al.[32]

Negligible sources of error include that due to the previously mentioned inexact knowledge of the distribution of initial velocities ($\sim\pm1\%$). The calculation of $F(\tau)$ was based on an assumption that the $F(\tau)$ for B^{12} formation at the center of the target layer accurately represented the average $F(\tau)$ for B^{12} formation throughout the target layer. The error in $F(\tau)$ due to such an assumption is less than $\pm1\%$. Another negligible source of error is that due to possible angular misalignment of the γ-ray detector ($<\pm1.1\%$ for a 0°–150° measurement).

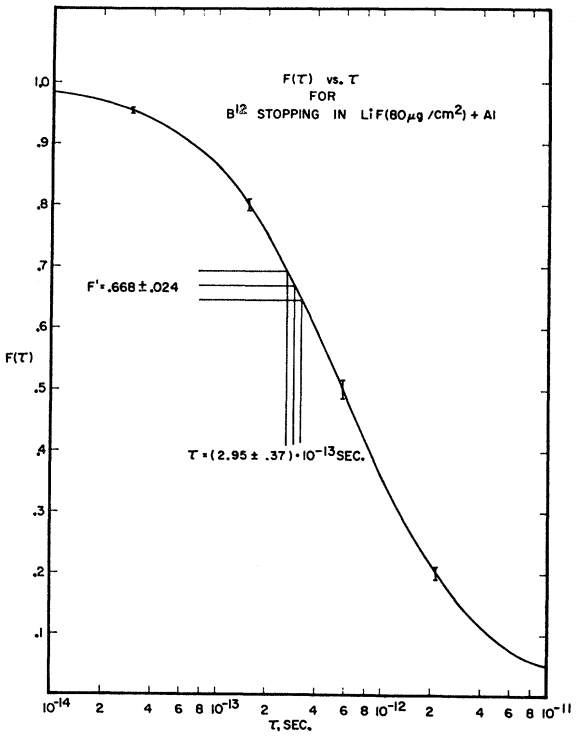

FIG. 3. $F(\tau)$ versus τ for B^{12} ions stopping in Li^7F (80 $\mu g/cm^2$) plus Al backing. The error bars on the solid curve refer to the uncertainty in $F(\tau)$ due to the $\pm7\%$ error estimate for the stopping-power data used.

Another possible source of error is that due to an assumption of an isotropic m_4-γ angular correlation and an isotropic angular distribution for reaction 2. A check on these assumptions, the angular distributions for reactions 1 and 3, and the lifetime result can be made by comparing the observed line shape with those calculated from the measured lifetime and angular-distribution data, with detector resolution and $dE_\gamma/d\theta_\gamma$ broadening folded in. The comparison is shown in Fig. 4. The line shape is strongly influenced by the angular distribution and correlation because of the considerable kinematical broadening present ($R=\beta_r/\beta_{c.m.}=$ 0.55 for reaction 1, for example). This may be seen from the almost identical 0° line shapes for lifetimes of 2.0, 3.0, and 4.0×10^{-13} sec. The 0° calculated line shape for 3.0×10^{-13} sec is in excellent agreement with the data. At 90° the fit is not as good, but the line broadening at 90° is relatively more sensitive to the detector resolution function, which was not well known for a 950-keV line in these spectra. The fit at 150° is good except for three rather badly scattered data points. It is, in fact, not possible to generate a fit to the 150° data which would be significantly better than that shown in Fig. 4. This follows from the fact that the Doppler broadening due to the lifetime is sufficiently extensive such that only a smoothly varying line shape can be expected, where a rapidly varying one is required for a better fit. The reasonably good fits obtained (Fig. 4) indicate that the assumptions of an isotropic angular correlation and isotropic angular distribution for reaction 2 are reasonable.

Finally, note that the lifetime result depends on the assumption that the lifetime of the B^{12} 2621-keV state is much shorter than that of the 953-keV state. It will be shown in Sec. IV that the 2621-keV-state lifetime is at least six times shorter than that of the 953-keV state. Such a limit on the 2621-keV-state lifetime, plus the fact that the 2621→953 transition provides only $(20\pm10)\%$ of the 953-keV-state population, indicates that the lifetime of the 2621-keV state is sufficiently fast to have a negligible effect on the 953-keV-state lifetime measurement.

A preliminary result [$\tau_m=(2.6\pm0.4)\times10^{-13}$ sec] was reported previously.[38] This result was calculated neglecting the detailed distribution of initial velocities and nuclear scattering effects. Thus the result quoted above, $\tau_m=(2.95\pm0.37)\times10^{-13}$ sec, is to be taken as the more reliable result.

The present result is in good agreement with, and substantially more accurate than, two previous determinations.[36] The averaged experimental value for the B^{12}(953) state lifetime has been compared elsewhere[36] with several theoretical predictions.

D. Lifetimes of the B^{11} 6.79- and 7.30-MeV States

B^{11} transitions from the 6.79- and 7.30-MeV states were observed in the Li^6+Li^6, Li^6+Li^7, and Li^7+Li^7 spectra. These spectra were accumulated for a variety of incident energies, backings, and γ-ray detector angles with respect to the beam axis. A particular case will be discussed here—the Li^6+Li^7 spectra for a Li^6 incident energy of 5.10 MeV, on a copper-backed 110-μg/cm^2 Li^7F target, with γ-ray detector angles of 0° and 90°. The regions of interest in the Li^6+Li^7 spectra are shown in Fig. 5.

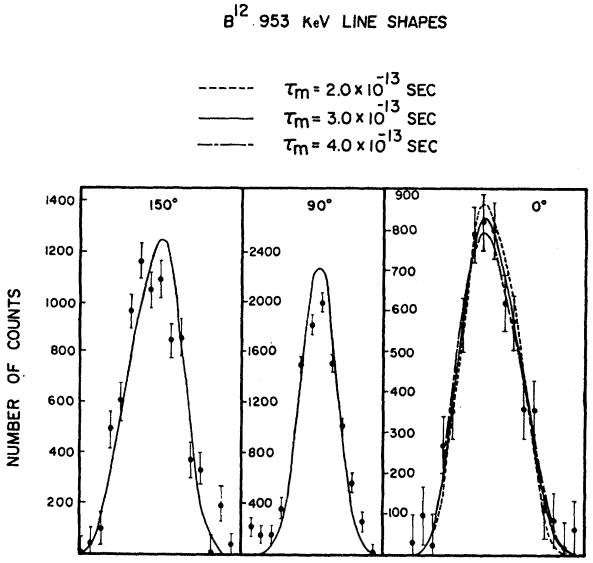

FIG. 4. Line shapes generated for the B^{12} 953-keV line from the Li^7+Li^7 spectrum. The shapes were calculated using the relative reaction contributions and angular distributions outlined in the text, assuming an isotropic angular correlation function. The shapes calculation for 90° and 150° are for a lifetime of 3.0×10^{-13} sec. The 0° line shapes are for lifetimes of 2.0, 3.0, and 4.0×10^{-13} sec. In the 0° case, the centroids of all three line shapes have been made to coincide with that of the data, for ease of comparison. The 2.0 and 4.0×10^{-13}-sec line-shape centroids actually would be expected to fall 0.8 channel above and below the 3.0×10^{-13}-sec line-shape centroid.

The possible reactions leading to the population of the B^{11} 6.79- and 7.30-MeV states are

(1) $Li^6+Li^7\rightarrow B^{11}(6.79, 7.30)+d$, $Q=+0.400, +0.110$ MeV

(2) $\rightarrow B^{11}(6.79, 7.30)+p+n$, $Q=-1.825, -2.115$ MeV.

The maximum kinematically allowed line broadening was considerably greater for reaction 1 (128 keV for the 7.30-MeV level) than for reaction 2 (48 keV for the same level), since the incident Li^6 energy was so near threshold for reaction 2. The observed broadenings of the 6.79- and 7.30-MeV lines are, in fact, approximately equal to those expected for reaction 1. Since ~80% of the counts in the 6.79- and 7.30-MeV lines fall outside the limits of broadening for reaction 2, at least 80% of the population of the corresponding levels is due to reaction 1. In addition, the observation of approximately full broadening for the 6.79- and

[38] M. J. Throop, Bull. Am. Phys. Soc. 12, 484 (1967).

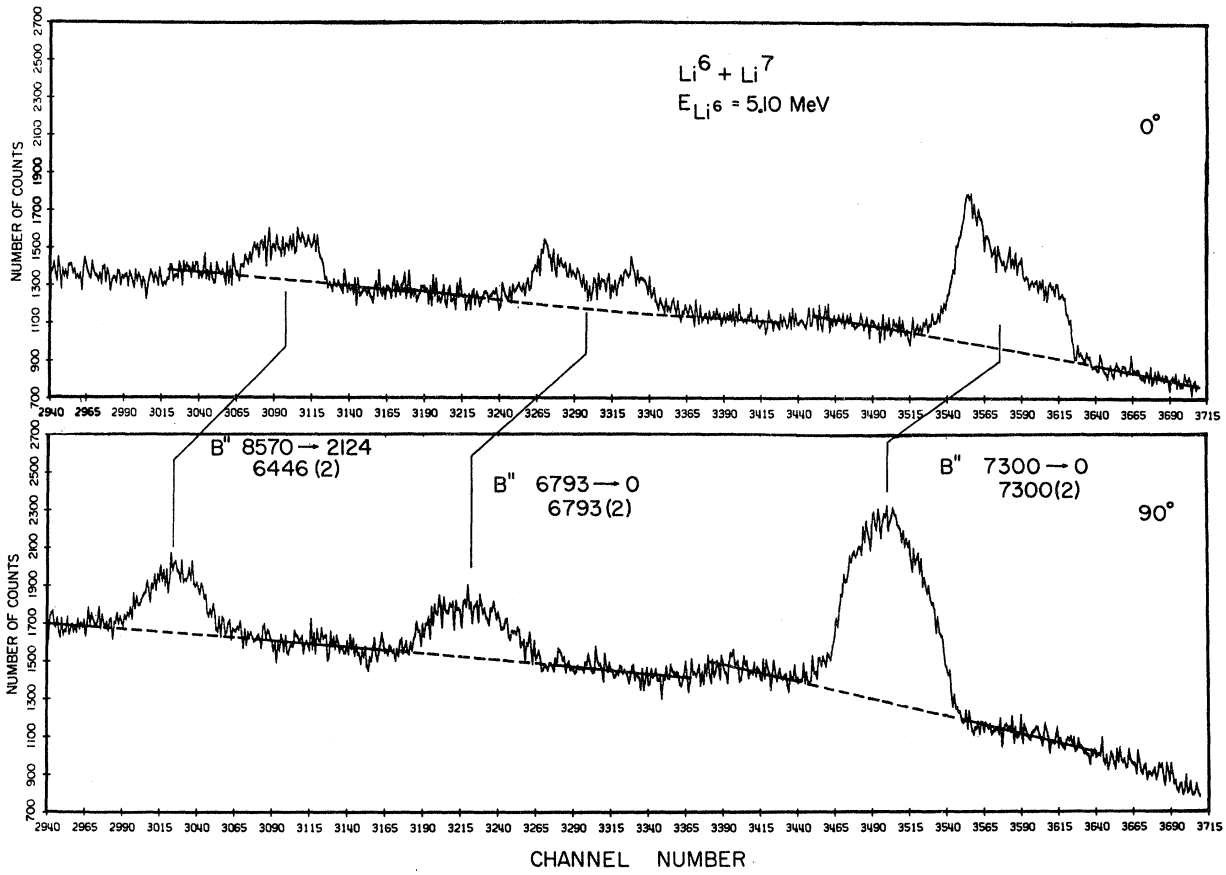

FIG. 5. Portion of the Li^6+Li^7 spectrum at $\theta_\gamma = 0°$ and 90° showing lines due to decay of the B^{11} 6793-, 7300-, and 8570-keV levels. The solid cruves on either side of the peaks are the best fit to the background region. The dashed lines under the peaks represent the background interpolated from the fit on either side of the peaks.

7.30-MeV lines implies lifetimes small compared to the stopping time of B^{11} in Li^7F and Cu.

The short lifetimes involved require accurate measurements of the nearly full shifts to be expected, and hence a careful subtraction of background underneath the peaks of interest. Some typical background subtraction problems are apparent upon examination of Fig. 5. These problems are of two types—those associated with a background which does not vary smoothly underneath the peak of interest and those associated with the correct separation of the peak (with possible tail) from the surrounding background.

Referring to Fig. 5 for an example of the first type of problem, it is seen that the 7.30-MeV two-escape peak has as part of its background the one-escape Compton edge of the 6.79-MeV line and the full-energy Compton edge of the 6.45-MeV line. The 7.30-MeV two-escape peak also has an energy nearly identical to that of a weak 6.79-MeV one-escape peak. The 6.79-MeV two-escape peak is sufficiently broad to be unresolvable from a relatively weak B^{11} 6.74-MeV-transition two-escape peak. It is clear that the background underneath the peaks of interest cannot simply be assumed to be flat. However, all the lines contributing to the background show approximately full Doppler broadening, so that the associated Compton edges, one-escape, and full-energy peaks are all broadened into a smoothly varying background. Also, the observation of approximately full Doppler broadening for all the transitions involved implies that to a good approximation the background shifts along with the peak of interest.

The background region used for subtraction purposes should ideally be outside the distribution of possible γ-ray energies for the the line of interest. Such a choice of background can be unduly restrictive for the case of very fast lifetimes. It is clear from the 0° spectrum of Fig. 5 that the background chosen for the peaks of interest extended into the region of possible decay energies. Such an extension was justified by the observation, for the peaks of interest, of approximately full Doppler broadening. For example, the 7.30-MeV line at 0° showed 100% of the kinematically allowed broadening within errors, implying a two-standard-deviation limit lifetime of $<0.28\times10^{-13}$ sec. Line shapes calculated for such a short lifetime were found to have a

low-energy tail which fell off very rapidly, leaving an insignificant fraction near the unshifted energy E_{γ_0}. This is to be expected for the initial m_4* velocities encountered in this work; a low-energy tail on the 0° line shape would be expected only if nuclear stopping and scattering were significant.

Note that the tails on the line shapes of Fig. 5 (both 0° and 90° spectra) are primarily due, not to lifetime effects, but to a detector resolution function which included an exponential tail. In practice, for lifetimes known to be fast from a broadening measurement, the background used extended up to the point where statistically significant deviations from the smooth trend of background points took place (Fig. 5).

That this subtraction procedure was correct for lifetimes $\leq 5\times10^{-14}$ sec was also verified in a measurement of the shift of the B^{11} 4.44–C^{12} 4.43-MeV line in the Li^7+Li^7 spectrum. From charged-particle cross-section data it is known that the B^{11} 4.44–C^{12} 4.43-MeV doublet is primarily due to the C^{12} transition. An attenuated shift was observed for this line, and the deduced C^{12} 4.43-MeV-level lifetime was in good agreement with the compiled value.

The soundness of the error estimates for the peak position due to background uncertainties was verified by observing that numerous transition energies (determined from the 90° spectrum) and Doppler-shift results showed a scatter entirely consistent with that expected from the error estimates.

The shifts observed for the 6.79- and 7.30-MeV transitions were 136.8±5.2 and 133.8±2.7 keV, respectively, leading to attenuation factors of 1.036± 0.130 and 1.003±0.120. These factors were determined using $R\langle\cos\theta_{c.m.}\rangle$ values extracted from angular-distribution data reported for reaction 1 at the same incident Li^6 energy.[34] The attenuation-factor errors include an error due to the unknown angular correlation function (±0.122 for the 6.79-MeV transition and 0.110 for the 7.30-MeV transition), as well as an error estimate due to possible angular misalignment of the γ-ray detector (±0.045 for a 0°–90° shift determination). The attenuation of the shift due to a finite detector solid angle was completely negligible compared to the above sources of error. The line-broadening attenuation factors were also determined from the 0° spectrum line shapes; these were 1.036±0.027 for the 6.79-MeV transition and 1.039±0.026 for the 7.30-MeV transition.

The portions of the Li^6+Li^7 spectra shown in Fig. 5 then provided the following lifetimes from shifts:

$$B^{11}(6.79):\quad \tau_m=(0.00_{-0.00}{}^{+0.54})\times10^{-13}\text{ sec}$$

$$B^{11}(7.30):\quad \tau_m=(0.00_{-0.00}{}^{+0.60})\times10^{-13}\text{ sec.}$$

The lifetime limits deduced from line-broadening measurements were consistent with these results.

Two additional sources of error in the lifetime result must be considered—those due to uncertainty in the stopping-power data and target thickness. The stopping-power-data uncertainty for the target and backing materials was ±7%. This propagates to a ±7% lifetime uncertainty. Several calculations for a range of target thicknesses showed that a ±25% variation in target thickness propagated to a ±4.5% error in the lifetime result. Both these sources of error contribute negligibly to the lifetime error compared to the $\langle\cos\theta_{c.m.}\rangle$ uncertainty.

It was noted previously that the calculations for F' and $F(\tau)$ did not include effects due to an azimuthally asymmetric distribution of the stopping media about the beam axis, where the distance traversed in the target material varied with the m_4* azimuthal angle. These effects were largest for lifetimes $\sim0.3\times10^{-13}$ sec, for which decays occurred about equally in the target and backing materials. For this range of lifetimes, the error introduced in the lifetime determination through neglect of asymmetric stopping effects was $<\pm4\%$. This error is again negligible compared to that introduced in the lifetime through the $\langle\cos\theta_{c.m.}\rangle$ uncertainty.

The lifetime results given above for the B^{11} 6.79- and 7.30-MeV states are typical of those obtained for a variety of reactions, γ-ray angles, and backings. An error-weighted average was performed for all the shift measurements. The line-broadening lifetime limits were used only as a check on the shift results and were not included in the averaging procedure. The final averaged lifetime limits and their significance are discussed in Sec. IV B.

E. Lifetime of the Ne^{20} First Excited State

The decay of the Ne^{20} 1632-keV state was observed in the Li^6+O^{16} spectra (Fig. 6). Spectra were accumulated for γ-ray detector angles of 30°, 90°, and 150° with respect to the beam axis at an incident Li^6 energy of 5.86 MeV. The target was 220-μg/cm² SiO evaporated on an aluminum backing. Angular-distribution data for deuteron groups to levels in Ne^{20} have been reported for the Li^6+O^{16} reaction at an incident energy of 5.88 MeV.[8] The possible modes by which the Ne^{20} 1632-keV level may be populated are

(1)	$Li^6+O^{16}\rightarrow Ne^{20}(1632)+d$,	$Q=1.627$ MeV
(2)	$\rightarrow Ne^{20}(1632)+p+n$,	$Q=-0.597$ MeV
(3)	$\rightarrow Ne^{20}(4250)+d$,	$Q=-0.791$ MeV
(4)	$\rightarrow Ne^{20}(4250)+p+n$,	$Q=-3.015$ MeV
(5)	$\rightarrow Ne^{20}(4970)+d$,	$Q=-1.511$ MeV
(6)	$\rightarrow Ne^{20}(4970)+p+n$,	$Q=-3.735$ MeV.

The 4250- and 4970-keV states decay 100% through the 1632-keV state. Note that F^{20}, which β decays to the Ne^{20} 1632-keV level, cannot be formed at the incident Li^6 energy used. Reactions 4 and 6 are ex-

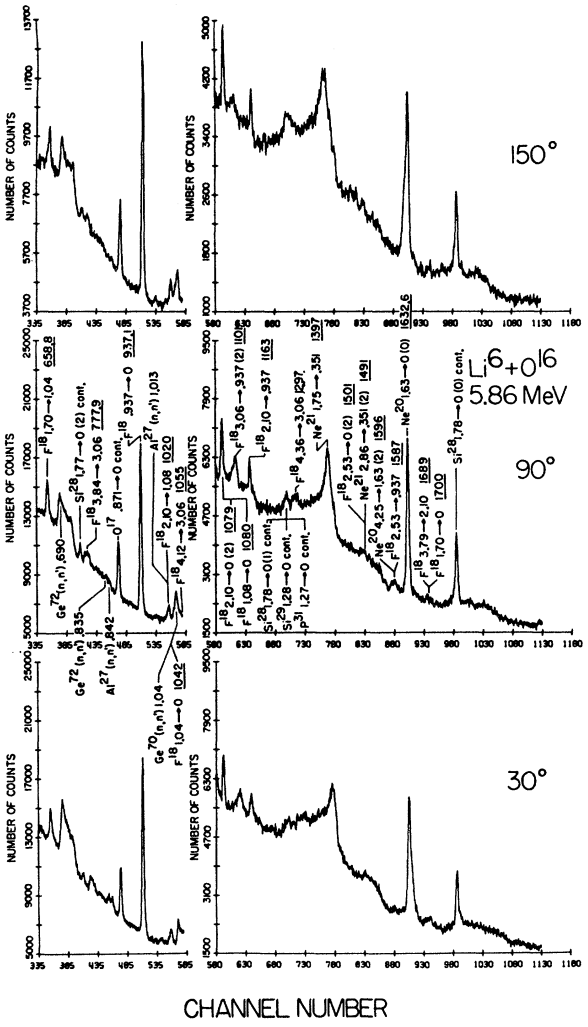

FIG. 6. Portion of the γ-ray spectra observed at $\theta_\gamma=30°$, 90°, and 150° in the 5.86-MeV Li^6 bombardment of a SiO target. Lines due to inelastic neutron scattering from Ge and Al are identified by the appropriate (n, n') reactions and the transition energy. Other lines in the $\theta_\gamma=90°$ spectrum are identified by the residual nucleus responsible for the transition and the energies of the initial and final states of the transition. The transition energy (minus 511 keV for one-escape peak, 1022 keV for two-escape peaks) is additionally listed for those lines due to the Li^6+O^{16} reaction. Lines which are not due to the Li^6+O^{16} reaction are considered contaminant lines and are denoted by the abbreviation CONT. Numerous transition energies (denoted by an underlined number) have previously been determined with some accuracy by other workers; many such energies were used as calibration points in a determination of the energies of other lines of interest. Full-energy, one-escape, and two-escape peaks are identified by (0), (1), and (2), respectively.

pected to be strongly suppressed relative to the others listed above, since only 1.2 and 0.5 MeV, respectively, were available to penetrate the 3.1-MeV Coulomb barrier for the p-Ne^{20} or p-Ne^{21} system.

The relative contributions to the population of the 1632-keV state were deduced from an analysis of γ-ray intensities, assuming that reactions 4 and 6 were of negligible magnitude, and using the available charged-particle reaction cross-section data. It found that reaction 1 contributed 8%, reaction 2 contributed 88%, reaction 3 contributed 1%, and reaction 5 contributed 3% to the population of the 1632-keV state. The errors on the reaction contributions are $\pm 5\%$.

No angular-distribution or -correlation data are available for the predominant reaction 2, so that some uncertainty was introduced in the calculated F' and $F(\tau)$. An estimated upper limit of ≤ 0.35 for $\langle\cos\theta_{c.m.}\rangle$ was given previously. This result led to a $\pm 16\%$ upper limit variation in F' due to uncertainty in the distribution of initial velocities.

Rather large zero shifts were encountered in the Li^6+O^{16} spectra. They were approximately as large as the centroid shift of the relatively long lived Ne^{20} 1632-keV state. The zero-shift correction was determined from a linear interpolation between the shifts of the 511-keV annihilation radiation line and the pulser peak. The corrected 30°–90° shift was $+2.33\pm 0.56$ channels and the 90°–150° shift was $+2.55\pm 0.56$ channels. The two results agree well within the quoted errors, as expected from the shift symmetry about $\theta_\gamma=90°$.

The centroid-shift result was then corrected for the contribution to the 1632-keV line from reaction 5. The 4970→1632-keV cascade γ-ray line was found to show no measurable shift. Thus it was possible to subtract the efficiency-corrected cascade peak from the channels centered about 1632 keV in the 30° and 150° spectra. This subtraction resulted in a 3% correction to the 1632-keV peak centroid shift.

The corrected 30°–150° shift was then obtained in keV using the dispersion (keV/channel) in the 1632-keV region determined from calibration lines in the Co^{60} and ThC'' spectra accumulated immediately after the last Li^6+O^{16} spectrum. $F(\tau)$ was calculated using the appropriate contributions for reactions 1 and 2 previously listed (reaction 3 was considered negligible and reaction 5 was corrected for as outlined above). Both F' and $F(\tau)$ were calculated assuming an isotropic angular distribution for reaction 2. The resulting lifetime, deduced from the centroid-shift measurement, was $\tau_m=1.55_{-0.40}{}^{+0.52}\times 10^{-12}$ sec, where the error is largely due to an inexact knowledge of $\langle\cos\theta_{c.m.}\rangle$.

A second more accurate determination of the Ne^{20} 1632-keV-state lifetime was based on a fit to the observed line shape. Such a determination does not depend on the accuracy of the zero-shift correction, and thus provides a check on it. In addition, for long lifetimes the line shape is relatively independent of the angular distribution and angular correlation functions.

Figure 7 is a comparison with the data of line shapes calculated for $\tau=1.0$, 1.2, and 1.6 psec, based on the relative amplitudes of reactions 1 and 2 listed previously, and assuming an isotropic angular distribution for reaction 2 as well as an isotropic angular correlation function for both reactions 1 and 2. It is clear from Fig. 7 that the centroid-shift-measurement result, $\tau\sim$

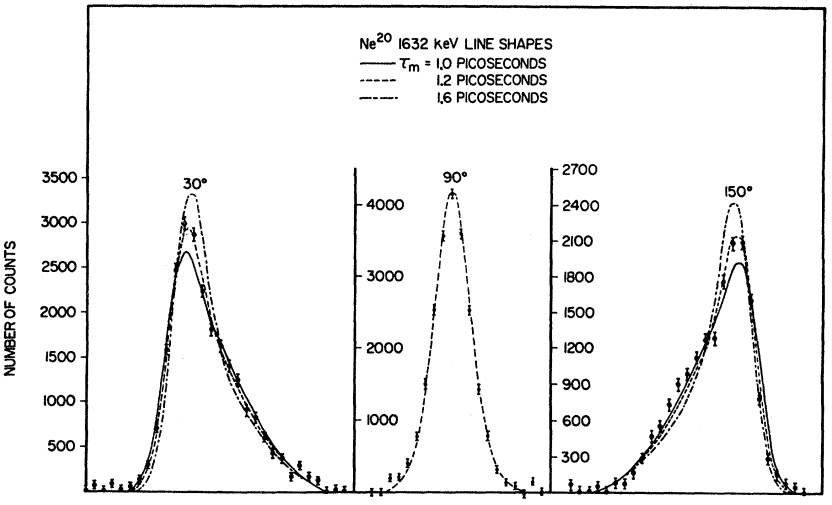

FIG. 7. Line shapes generated for the Ne^{20} 1632-keV line in the Li^6+O^{16} spectrum. The line shapes were calculated using the relative reaction contributions and angular distributions outlined in the text, assuming an isotropic angular correlation function. The line shapes for lifetimes of 1.0, 1.2, and 1.6 psec are shown with the $\theta_\gamma=30°$ and 150° data. The centroids of the three line shapes have been made to coincide with that of the data for ease of comparison. The centroid shift at $\theta_\gamma=30°$ and 150° should actually be increased by 1.8 and 1.0 channels for the 1.0- and 1.2-psec line shapes. At $\theta_\gamma=90°$ only the 1.2-psec line shape is shown; the 1.0- and 1.6-psec line shapes are virtually identical to the 1.2-psec line shape.

1.6 psec, leads to a line shape which fits the data poorly. In fact, because the line shape is nearly independent of the angular-distribution–angular-correlation function, it was not possible to find a reasonable angular distribution which, together with a 1.6-psec lifetime, gave a good fit to the data. Such an inconsistency implied an inaccuracy in the zero-shift correction to the centroid-shift measurement.

An excellent fit to the data was obtained for a 1.2-psec lifetime and an isotropic angular distribution for reaction 2 (as shown in Fig. 7). A search was made for other lifetime–angular-distribution combinations which might also fit the data. Satisfactory fits were obtained for a lifetime of 1.0 and 1.4 psec, assuming reaction-2 angular distributions corresponding to the most extreme backward and forward peaking, respectively, allowed by the $\langle\cos\theta_{c.m.}\rangle$ limits.

The resulting Ne^{20} 1632-keV-state lifetime, from analysis of the line shape, is $\tau_m=(1.20\pm0.20)\times10^{-12}$ sec, where the error limits correspond to the range of lifetimes over which an adequate fit to the data could be achieved, assuming reasonable angular distributions.

For long lifetimes the line shape is strongly influenced by the detector resolution function, which may include broadening due to zero- or gain-shift effects. Thus the detector resolution function must be accurately determined for each spectrum. The Li^6+O^{16} spectra contain several strong lines due to long-lived states, for example, the O^{17} 871- and F^{18} 937-keV lines, as well as annihilation radiation. It was found that a Gaussian function with a FWHM of 7.12 keV gave an excellent fit to the sharp lines for all three angles of γ-ray observation. That the detector resolution function was correctly determined may be seen from the good fit obtained for the 1632-keV peak at $\theta_\gamma=90°$, where the peak shape is more sensitive to the detector resolution function than to lifetime effects.

Other sources of error which can be considered negligible are those due to a $\pm5\%$ quoted error for the electronic stopping power of Ne^{20} in Al and a $\pm20\%$ uncertainty in the nuclear stopping power.[39] Each of these uncertainties leads to a $\pm4\%$ variation in τ, which is small compared to the error in τ due to the lack of knowledge of the angular distribution for reaction 2. The variation of the results of the centroid-shift measurement or the line-shape fit with the choice of region used in the background fit was found to be negligible. The effect of a possible $\pm25\%$ variation in the target thickness on the lifetime result was completely negligible, since the long Ne^{20} lifetime ensured that most decays occur in the backing and, in addition, the SiO target and Al backing had nearly identical stopping-power characteristics.

Since the centroid-shift and line-shape lifetime results overlap, the weighted average has been taken, giving $\tau_m=1.26\pm0.24$ psec.

IV. RESULTS

A. B^{10}

Transitions were observed in the Li^6+Li^6 (Fig. 8) and Li^6+Li^7 spectra. The lifetime of the 2.15-MeV level was determined from the shift of the 0.414-MeV branch to the 1.74-MeV level (not shown in Fig. 8). A weighted average of two measurements gave a result of $\tau_m=1.27_{-0.34}^{+0.53}$ psec. This result is in fair agreement with that reported by Donohue and co-workers[40] and in poor agreement with that of Fisher and co-workers.[41]

The lifetime of the 3.59-MeV level was determined from both the 3.59→0- and 3.59→0.717-MeV transitions (see Fig. 8). The weighted average of three measurements was $\tau_m=(1.00\pm0.30)\times10^{-13}$ sec, which

[39] A. E. Blaugrund, D. H. Youngblood, G. C. Morrison, and R. E. Segel, Phys. Rev. **158**, 893 (1967).
[40] D. J. Donohue, M. J. Wozniak, R. L. Hershberger, J. E. Cummings, and J. A. Lonergan, Phys. Rev. **165**, 1071 (1968).
[41] T. R. Fisher, S. S. Hanna, and P. Paul, Phys. Rev. Letters **16**, 850 (1966).

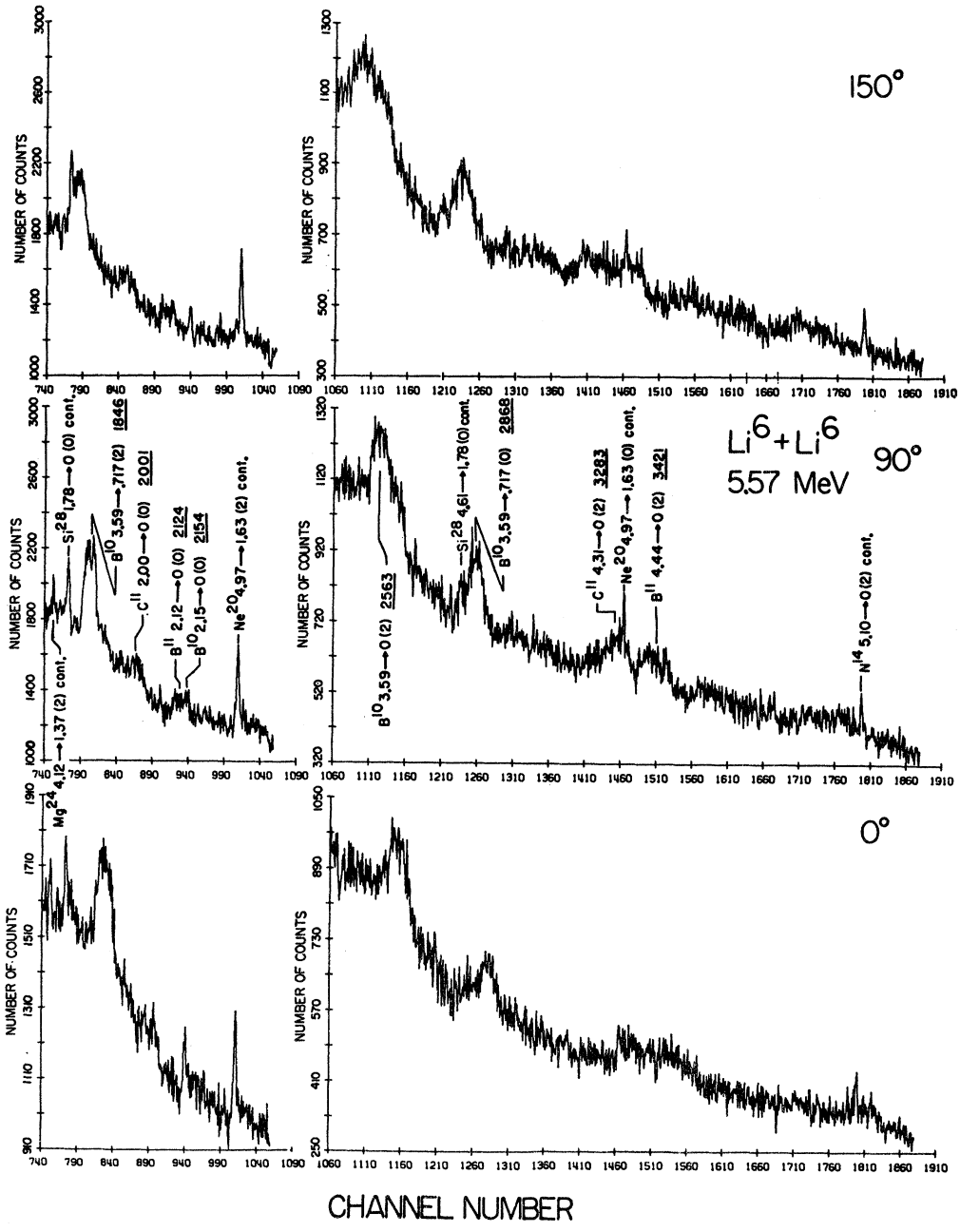

FIG. 8. Portion of the γ-ray spectra observed at $\theta_\gamma = 0°$, 90°, and 150° in the 5.57-MeV Li^6 bombardment of a Li^6F target. The presentation is identical to that of Fig. 6.

falls within the quoted errors of three previously reported determinations.[40–42]

B. B^{11}

Transitions were observed in the Li^6+Li^6 (Fig. 9), Li^6+Li^7 (Fig. 5), Li^7+Li^7, Li^7+Be^9 (Fig. 10), and Li^6+B^{10} spectra.

Numerous shift and broadening measurements were made for transitions to the ground and in some cases to the 2.14-MeV state from the B^{11} 6.74-, 6.79-, 7.28-, 7.98-, and 8.56-MeV states. Measurements of the shift and energy at $\theta_\gamma = 90°$ for the B^{11} 8.92-MeV state were also made. The results for this state are in agreement with its known lifetime and excitation energy,[42] and serve as a partial check on the methods used in the present work.

[42] E. K. Warburton, J. W. Olness, K. W. Jones, C. Chasman, R. A. Ristinen, and D. H. Wilkinson, Phys. Rev. **148**, 1072 (1966).

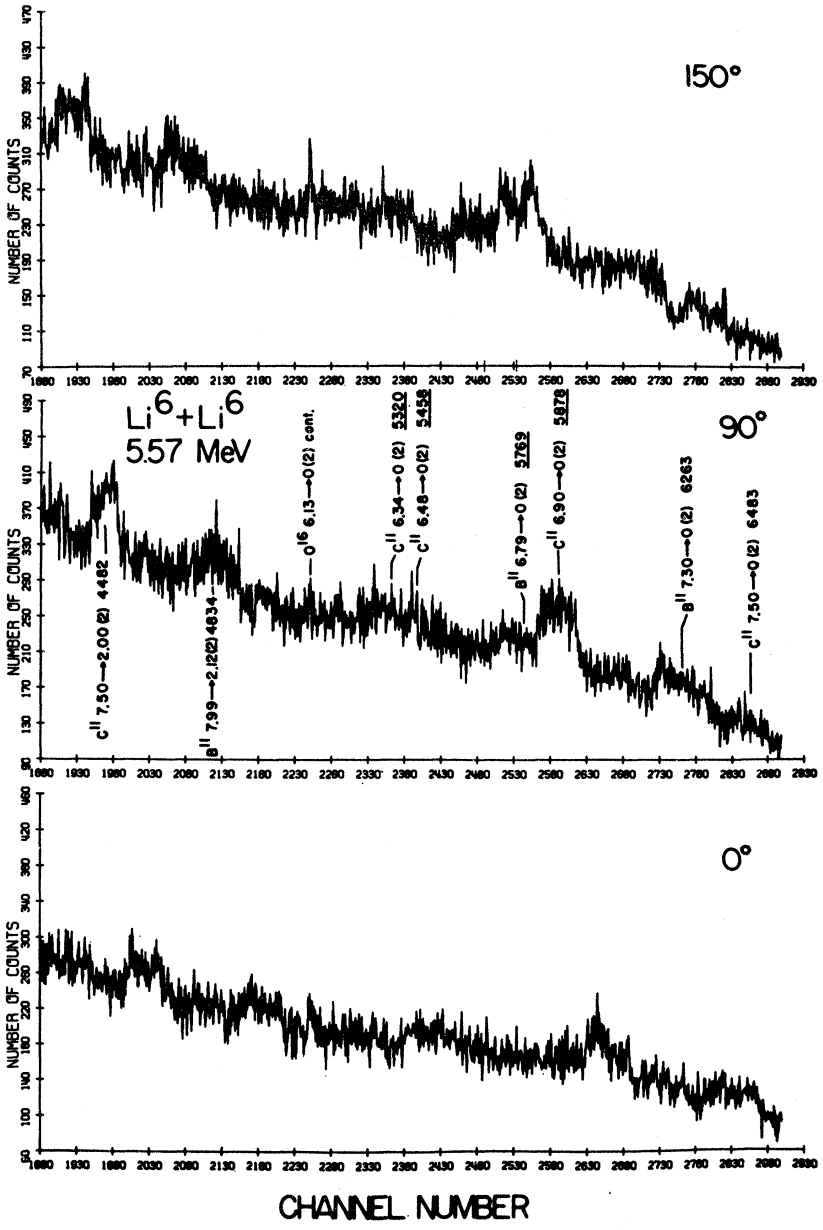

FIG. 9. Portion of the γ-ray spectra observed at $\theta_\gamma=0°$, 90°, and 150° in the 5.57-MeV Li^6 bombardment of a Li^6F target. The presentation is identical to that of Fig. 6.

All the shift-attenuation-factor results fell well within two standard deviations of unity (full shift). The resulting error-weighted average lifetime limits are, to two standard deviations,

B^{11} 6.74 MeV,	$\tau_m<2.1\times10^{-13}$ sec,
6.79 MeV,	$<0.35\times10^{-13}$ sec,
7.28 MeV,	$<0.23\times10^{-13}$ sec,
7.98 MeV,	$<0.66\times10^{-13}$ sec,
8.56 MeV,	$<0.60\times10^{-13}$ sec.

Each result is based on at least five measurements. The limit obtained for the 6.74-MeV state is comparable to the three-standard-deviation limit of 3.0×10^{-13} sec reported by Warburton *et al.*[42] A limit has not previously been reported for the 6.79-MeV level. The limits for the last three states listed above are considerable improvements over the previously reported limits of $<1.0\times10^{-13}$ sec for the 7.28-[42] and $<5.0\times10^{-13}$ sec for the 7.98- and 8.56-MeV states.[22] γ-ray decay widths from inelastic electron scattering have been reported for the 7.28- and 8.56-MeV states.[43,44] Although

[43] R. D. Edge and G. A. Peterson, Phys. Rev. **128**, 2750 (1962).
[44] E. Spamer, Z. Physik **191**, 24 (1966).

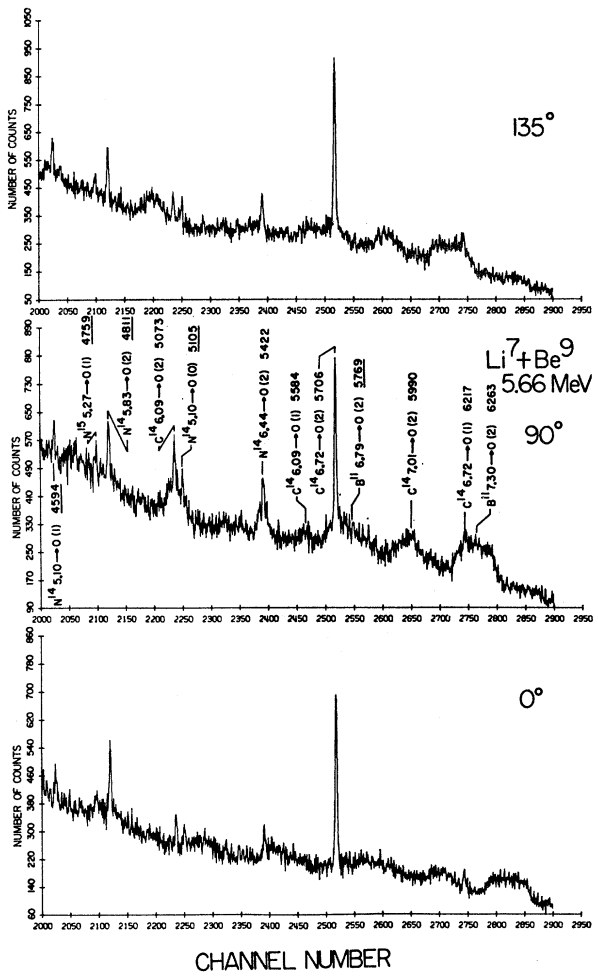

FIG. 10. Portion of the γ-ray spectra observed at $\theta_\gamma=0°$, 90°, and 135° in the 5.66-MeV Li^7 bombardment of a Be target. The presentation is identical to that of Fig. 6.

implying much lower limits than the present work, the inelastic electron scattering results are somewhat model-dependent. The 6.79- and 7.28-MeV-state limits listed above are lower than the $<0.4\times10^{-13}$-sec three-standard-deviation limits given in a preliminary report of this work.[38] In the case of the 7.98-MeV state, the limit reported here is somewhat larger, primarily because of more conservative error estimates.

The limits reported here do not lead to any revisions of spin and parity assignments or new values for transition multipolarities in B^{11}; however, they are useful for planning further lifetime measurements.

Recently precise measurements of level energies in B^{11} below 7 MeV[45] resulted in excitation energies 10–20 keV lower than previously compiled energies.[22] In the present work, γ-ray energies (which can be converted to excitation energies by adding the nuclear recoil correction of a few keV) were measured for the 7.28-, 7.98-, and 8.56-MeV levels of B^{11}. The energy calibration used depended on the accurate excitation energies reported for levels below 7 MeV.[45] As is clear from Table II, the summarized γ-ray energy results for levels in B^{11} above 7 MeV continue the trend of being 10–20 keV less than the previously accepted values.

C. B^{12}

Transitions were observed and analyzed for the Li^7+Li^7 spectra (Fig. 1). The determination of the B^{12} 953-keV-level lifetime was outlined in some detail in Sec. III. The only other B^{12} transitions observed were the ground-state decay from the 1674-keV level and decay from the 2621-keV level via the 2621→953-keV branch. These two Doppler-broadened lines (1668 and 1674 keV) were unresolved. An analysis of charged-particle and γ-ray intensity data as outlined in Sec. III showed that the two members of the unresolved doublet must be about equal in intensity. Recent measurements[46] for the B^{12} 1674-keV state indicate a lifetime of <20 fsec. This upper limit is sufficiently short to allow the limit derived from the doublet shift to be referred entirely to the lifetime of the 2621-keV level. The resulting lifetime limit (to two standard deviations) is $\tau_m<0.48\times10^{-13}$ sec. This is short enough to ensure a negligible effect on the lifetime of the 953-keV level through cascade feeding from the 2621-keV level.

Comparison of the experimental lifetimes and limits (including the results reported here) with theoretical predictions for B^{12} transitions have been made elsewhere.[36]

D. B^{13}

Transitions observed in the Li^7+Li^7 spectra (Fig. 11) were the ground-state decays from the 3.53-, 3.71-, and 4.13-MeV states. Only the 4.13-MeV line was sufficiently well defined to permit a quantitative lifetime measurement; for the 3.53- and 3.71-MeV levels limits of >3.0 and $<3.8\times10^{-13}$ sec were set. The 4.13-MeV level may have a measurable lifetime [$\tau_m=(0.62\pm0.50)\times10^{-13}$ sec weighted average over two measurements], although the rather large errors in the results do not preclude a very fast lifetime. Possible spins of $\frac{1}{2}^-$, $\frac{5}{2}^-$, and $\frac{7}{2}^-$ have been suggested for the 4.13-MeV state from B^{11} (t, p) angular-distribution data.[47] Although spins of $\frac{1}{2}$ or $\frac{5}{2}$ cannot be ruled out, the shift-measurement indication of a lifetime not much faster than 10^{-14} sec, combined with the reported 25% branch to the 3.48–3.53-MeV doublet in competition with a 75% ground-state branch,[48] suggests a spin assignment of $\frac{7}{2}$ for the 4.13-MeV level, given a ground-state spin of $\frac{3}{2}^-$. Spins of $\geq\frac{7}{2}$ for the 3.53- and $\leq\frac{5}{2}$

[45] C. P. Browne and F. H. O'Donnell, Phys. Rev. **149**, 767 (1966).

[46] M. J. Throop (to be published).

[47] R. Middleton and D. J. Pullen, Nucl. Phys. **51**, 50 (1964).

[48] R. R. Carlson and E. Norbeck, Phys. Rev. **131**, 1204 (1963).

for the 3.71-MeV states are consistent with the lifetime limits obtained.

Transition energies for 3.53- and 4.13-MeV-level ground-state decays were determined (see Table II). The results are in good agreement with values determined from $B^{11}(t, p)$ measurements.[47]

E. C^{11}

Transitions were observed in the Li^6+Li^6 spectra (Figs. 8 and 9). An estimated two-standard-deviation limit of 5×10^{-13} sec was made for each state contributing to the unresolved C^{11} 6.34–6.48-MeV doublet. Except for the 7.50-MeV-state transitions to the ground and first excited states, other observed transitions in C^{11} were members of unresolved C^{11}–B^{11} doublets. Thus the lifetime limits from shift measurements for the C^{11} 4.31- and 6.90-MeV levels are dependent on a knowledge of the lifetimes of the B^{11} 4.44- and 6.79-MeV states contributing to the B^{11} members of each doublet. Since the limits on the lifetimes for the B^{11} states (see Sec. IV B) are much smaller than the limits obtained for the B^{11}-C^{11} doublets, the doublet limits have been taken as applying to the C^{11} lifetimes alone.

The weighted-average lifetime two-standard-deviation limits obtained were

C^{11} 4.31 MeV, $\tau_m<1.4\times10^{-13}$ sec,
6.34 MeV, $<5.0\times10^{-13}$ sec,
6.48 MeV, $<5.0\times10^{-13}$ sec,
6.90 MeV, $<0.69\times10^{-13}$ sec,
7.50 MeV, $<0.91\times10^{-13}$ sec.

Each result is based on at least two measurements. The limits established in this work are lower than those previously reported for the C^{11} 4.31-, 6.90-, and 7.50-MeV states[13,42] and higher than those reported for the 6.34- and 6.48-MeV levels.[42]

F. C^{13}

Transitions were observed in the Li^6+Be^9 and Li^7+B^{11} (Fig. 12) spectra. No significant lifetime information was obtained for C^{13} levels.

Accurate transition-energy results were obtained for the 3.09- and 3.85-MeV levels. The result for the 3.85-MeV level is based on 22 measurements of the energy difference between the 3.68- and 3.85-MeV ground-state transition peaks. The result for the 3.85–3.68-MeV energy difference was 169.63±0.23 keV, in excellent agreement with a previous determination of 169.5±0.5 keV.[22] The 3.85-MeV ground-state transition energy (Table II) was obtained from the above difference and an accurate ground-state transition energy reported for the 3.68-MeV level.[49]

[49] W. V. Prestwich, R. E. Coté, and G. E. Thomas, Phys. Rev. **161**, 1080 (1967).

TABLE II. Summary of lifetime and transition-energy measurements.

Nucleus, level	τ_m (10^{-13} sec)	$E_{\gamma 0}$[a]
B^{10}(2.15)	$12.7_{-3.4}{}^{+5.3}$	...
B^{10}(3.59)	1.00±0.30	...
B^{11}(6.74)	<2.1	...
B^{11}(6.79)	<0.35	...
B^{11}(7.28)	<0.23	7284.6±2.2
B^{11}(7.98)	<0.66	7978.5±2.7
B^{11}(8.56)	<0.60	8556.5±3.3
B^{12}(0.953)	2.95±0.37	...
B^{12}(2.62)	<0.48	...
B^{13}(3.53)	>3.0	3536.3±4.2
B^{13}(3.71)	<3.8	...
B^{13}(4.13)	0.62±0.50	4133.4±7.8
C^{11}(4.31)	<1.4	...
C^{11}(6.90)	<0.69	...
C^{11}(7.50)	<0.91	7505±8
C^{13}(3.09)	...	3084.2±2.0
C^{13}(3.85)	...	3853.57±0.28
C^{14}(6.09)	<3.2	6094.5±3.2
C^{14}(6.72)	...	6728.1±1.4
C^{14}(7.01)	<1.2	7011.7±5.2
N^{14}(3.95)	...	1631.3±1.3 (3.95→2.31)
N^{14}(4.91)	...	4913.8±3.0
N^{14}(6.20)	...	3883.0±1.9 (6.20→2.31)
N^{14}(6.44)	6.3±0.8	6443.7±1.8
N^{15}(9.83)	<1.9	4562.6±4.0 (9.83→5.27)
N^{16}(0.298)	>7	297.6±0.9
N^{16}(0.398)	>9	397.8±1.0
		276.2±0.8 (0.398→0.122)
N^{17}(1.37)	<2	1370.7±0.8
N^{17}(1.91)	>5	1908.0±0.8
N^{17}(2.53)	...	619.9±3.5 (2.53→1.91)
N^{17}(3.13)	<3	1226.2±4.5 (3.13→1.91)
N^{17}(3.22)	>3	3222.0±7.1
N^{17}(3.67)	...	531.4±4.6 (3.67→3.13)
O^{16}(8.87)	3.7±1.3	2740.4±1.0 (8.87→6.13)
O^{18}(1.98)	...	1982.3±0.8
O^{18}(3.55)	...	1571.9±2.5 (3.55→1.98)
O^{18}(3.63)	...	1649.8±2.2 (3.63→1.98)
O^{18}(3.92)	...	1938.6±2.1 (3.92→1.98)
F^{18}(4.36)	<6.1	1297.4±2.5 (4.36→3.06)
Ne^{20}(1.63)	12.7±2.4	...
Ne^{21}(5.33)	<7	...
Ne^{21}(5.62)	<7	...
Ne^{21}(5.77)	<7	...
Ne^{21}(5.99)	<7	...
Ne^{21}(6.26)	<7	...
Ne^{21}(6.74)	<7	...

[a] Unless otherwise noted, transition energy refers to ground-state transition.

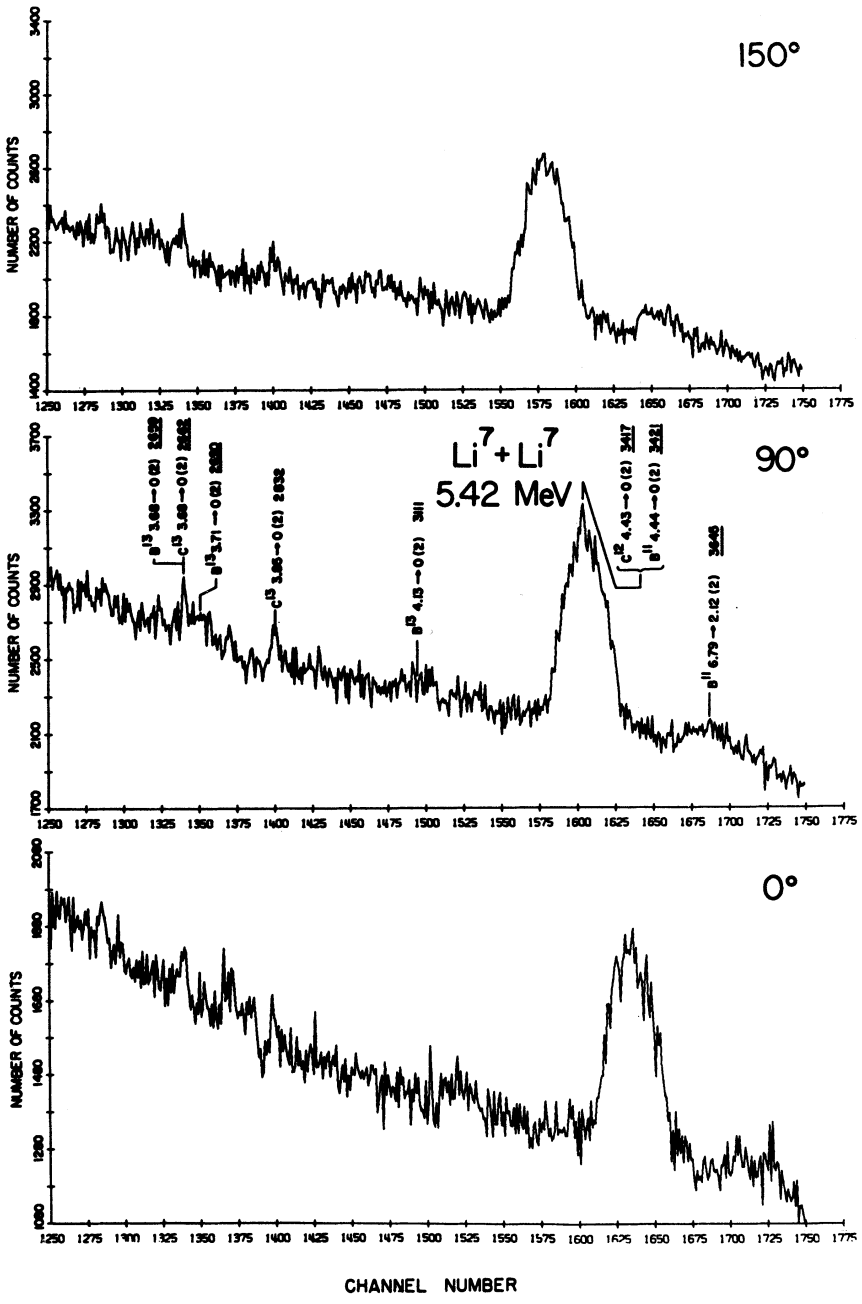

FIG. 11. Portion of the γ-ray spectra observed at $\theta_\gamma=0°$, 90°, and 150° in the 5.42-MeV Li^7 bombardment of a Li^7F target. The presentation is identical to that of Fig. 6.

G. C^{14}

Transitions were observed in the Li^7+Be^9 (Fig. 10) spectra. Only the ground-state decays of the 6.09-, 6.72-, and 7.01-MeV levels were observed. The 6.09-MeV line had a nonshifting component which could be attributed entirely to a branch from the long-lived 6.72-[50] to the 6.09-MeV state. The sharp 6.09-MeV component could thus be accurately subtracted from the 6.09-MeV broadened line shape. The resulting error-weighted average lifetime limits for the 6.09- and 7.01-MeV levels, to two standard deviations, were

$$C^{14}\ 6.09\ \text{MeV}, \quad \tau_m<3.2\times10^{-13}\ \text{sec},$$

$$C^{14}\ 7.01\ \text{MeV}, \quad \tau_m<1.2\times10^{-13}\ \text{sec}.$$

Each result is based on four measurements. The lifetime limit for the 6.09-MeV transition is nearly the same as one previously reported.[50] No limit has previously been reported for the 7.01-MeV level. The

[50] D. E. Alburger, A. Gallmann, J. B. Nelson, J. T. Sample, and E. K. Warburton, Phys. Rev. **148**, 1050 (1966).

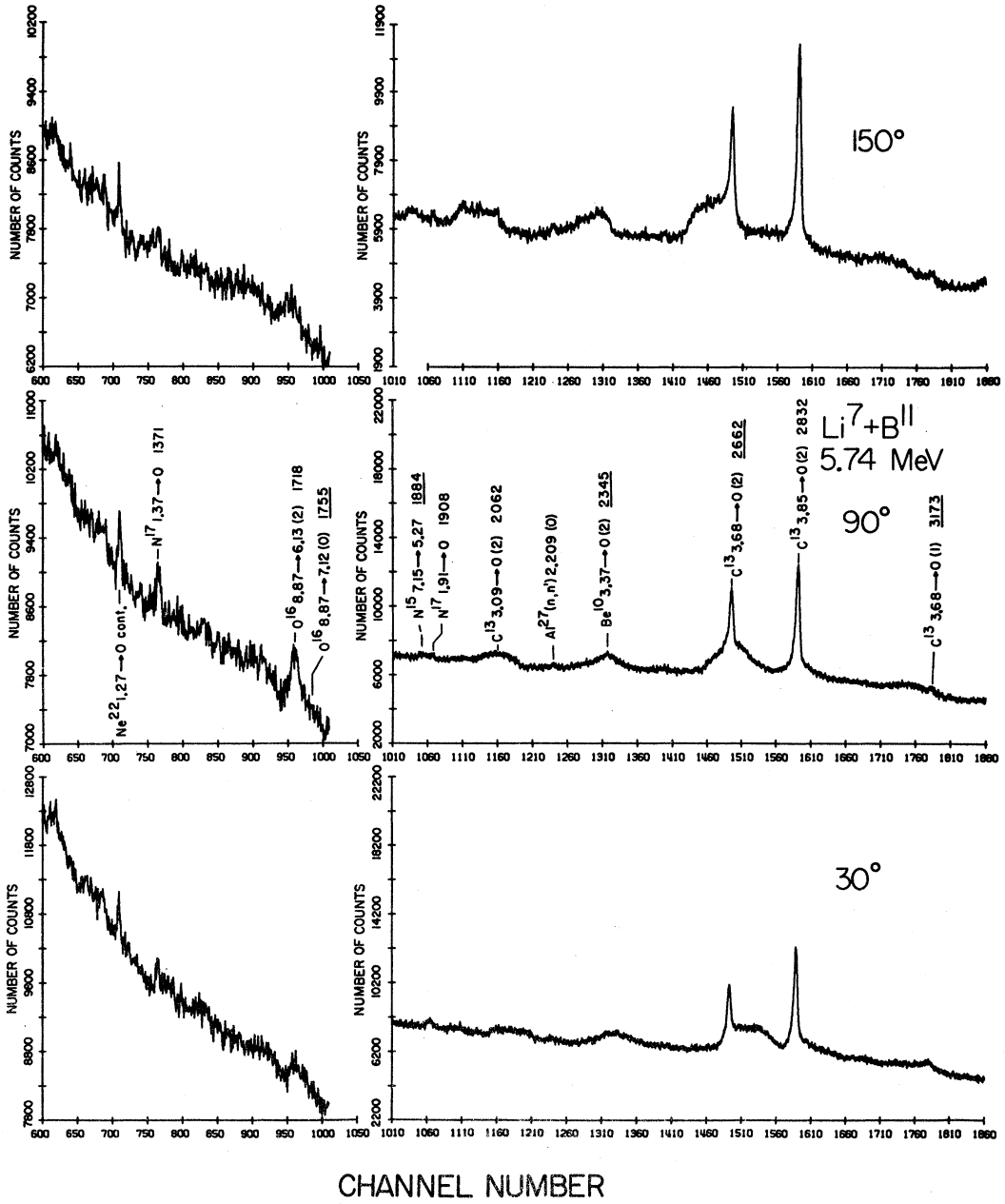

FIG. 12. Portion of the γ-ray spectra observed at $\theta_\gamma = 30°$, 90°, and 150° in the 5.74-MeV Li^7 bombardment of a B^{11} target. The presentation is identical to that of Fig. 6.

present limit is consistent with the probable spin and parity assignment of 2^+.[50] Certainly any higher spin can be ruled out by the lifetime limit set here.

The 6.09-, 6.72-, and 7.01-MeV ground-state transition energies were also obtained. These were 6094.5±3.2, 6728.1±1.4, and 7011.7±5.2 keV, and are in good agreement with the values determined from compiled excitation energies.[22] A knowledge of the 6.09-MeV excitation energy permits accurate excitation energies to be obtained for the 6.59-, 6.89-, and 7.32-MeV levels using the accurate energies[50] determined for the transitions from these levels to the 6.09-MeV level.

H. N^{14}

Transitions were observed and analyzed in the Li^6+Be^9, Li^7+Be^9 (Fig. 10), Li^6+B^{10}, and Li^6+C^{12} spectra. The resulting weighted-average lifetime result for the N^{14} 6.44-MeV level was

$$N^{14}\ 6.44\ \text{MeV}, \qquad \tau_m = (6.3 \pm 0.8) \times 10^{-13}\ \text{sec}.$$

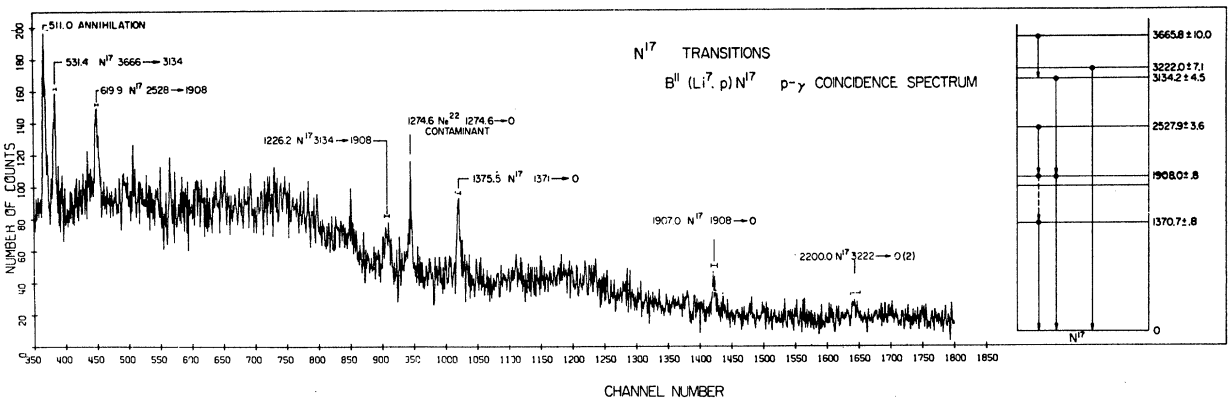

FIG. 13. Spectrum of N^{17} γ-rays observed at $\theta_\gamma = 90°$ in coincidence with protons ($\theta_{lab} = 140° \pm 22.5°$) from the $B^{11}(Li^7, p)N^{17}$ reaction. The 511-keV annihilation radiation line is from accidental coincidences and the Ne^{22} 1274.6-keV line is from the $O^{16}(Li^7, p)Ne^{22}(1274)$ contaminant reaction. The transitions observed and the deduced energies of N^{17} levels are shown in the energy-level diagram on the right. The bars above each peak show the maximum kinematically allowed Doppler broadening for the transition.

This result, based on 12 measurements, is in good agreement with a previous determination of $(5.9 \pm 1.2) \times 10^{-13}$ sec for the 6.44-MeV level.[51]

Transition energies were also obtained. These were, for the 3.95→2.31-MeV transition, 1631.3±1.3, for the 4.91→0-MeV transition, 4913.8±3.0, for the 6.20→2.31-MeV transition, 3883.0±1.9, and for the 6.44→0-MeV transition, 6443.7±1.8 keV. These results are in good agreement with, but more accurate than, those derived from compiled excitation energies.[22]

I. N^{15}

Transitions were observed in the Li^7+C^{12} and C^{13} spectra. The Q values for both the Li^7+C^{12} and Li^7+C^{13} reactions were such as to permit large recoil fractions in vacuum for most N^{15} levels. A significant lifetime limit was obtained for the N^{15} 9.83-MeV level, for which the vacuum recoil was nearly negligible. The relative contributions of the Li^7+C^{12} and Li^7+C^{13} reactions were not known, so that the lifetime limit was calculated using the larger maximum kinematically allowed shift for the Li^7+C^{12} reaction. The resulting two-standard-deviation limit of $<1.9\times10^{-13}$ sec is somewhat faster than a previously reported limit for the N^{15} 9.83-MeV level.[25] The 9.83→5.27-MeV transition energy (Table II) is in fair agreement with that deduced from previously reported excitation energies.[25]

J. N^{16}

Transitions from the 398- and 298-keV levels were observed in the Li^7+B^{11} spectra. No consistent shift or Doppler broadening could be observed for transitions from these levels. Two-standard-deviation limits of >0.9 and >0.7 psec were set for the 398- and 298-keV levels. Lifetime limits have not previously been reported for the N^{16} 398- and 298-keV levels. The present limits are consistent with the known spins and branching ratios for these levels.[22]

The transition energies were determined by comparison with the position of accurately known ThC″ calibration spectrum lines at 277 and 300 keV[52] after correction for a small zero shift between the calibration and Li^7+B^{11} spectra. The zero-shift correction was made by monitoring the position of the 511-keV line appearing in all the spectra. The resulting N^{16} excitation energies are 121.6±1.3, 297.6±0.9, and 397.8±1.0 keV. These results are in good agreement with, but more accurate than, previously compiled values.[22]

K. N^{17}

Transitions were observed in the Li^7+B^{11} spectra. Two types of spectra, singles (Fig. 12) and proton-γ coincidence (Fig. 13), were obtained.

The essential features of the coincidence geometry were outlined in the Sec. II. The coincidence spectrum was a spectrum of γ rays coincident with proton groups to all bound levels of N^{17}, so that background due to γ-ray transitions in nuclei other than N^{17} was supressed. The reduction of background permitted the observation of numerous weak N^{17} lines not discernible in the singles spectra. The mean N^{17} recoil angle for the coincidence geometry was 75° with respect to the γ-ray detector axis. Thus lines in the coincidence spectrum were expected to be shifted somewhat from the E_{γ_0} value, depending on the lifetimes of the states contributing, through direct population or cascade, to the transition. Such possible shifts were, for example, a maximum of +6.7 keV for the 1.37→0-MeV transition and +15 keV for the 3.22→0-MeV transition. Additionally, Doppler broadening due to finite particle and γ-ray detector solid angles could be expected for the fast transitions.

[51] J. A. Becker and E. K. Warburton, Phys. Rev. **134**, B349 (1964).

[52] C. M. Lederer, J. M. Hollander, and I. Perlman, *Table of Isotopes* (John Wiley & Sons, Inc., New York, 1967), 6th ed.

The maximum allowed broadenings are indicated in Fig. 13.

The assignment of observed lines to transitions in N^{17} was based on a previous study of proton-γ coincidence spectra for N^{17} produced in the $B^{11}(Li^7, p)$ reaction.[53] Transitions from levels up to 3.67 MeV in N^{17} were of sufficient intensity to be clearly observed.

It is clear that results obtained from the analysis of shift and broadening results were in the form of lifetime limits, since the shift and broadening of observed transitions from the states below 3.67 MeV were determined in part by the lifetimes of levels possibly feeding these states through transitions too weak to be observed. The lower-limit lifetimes obtained for the 1.91→0- and 3.22→0-MeV transitions are based on the lack of broadening observed for these lines in the two types of spectra. The 1.91→0-MeV transition was not broadened, even though fed by a broadened 3.13→1.91-MeV transition. The 3.22→0-MeV transition was not broadened, and no evidence could be found for feeding from higher levels. The resulting lifetime limits, to two standard deviations, were

N^{17} 1.37 MeV, $\tau_m < 2\times10^{-13}$ sec,
1.91 MeV, $> 5\times10^{-13}$ sec,
3.13 MeV, $< 3\times10^{-13}$ sec,
3.22 MeV, $> 3\times10^{-13}$ sec.

The possible broadening was too small to detect for transitions from the 2.53- and 3.67-MeV levels, and so no lifetime limits were obtained.

The excitation energies obtained for N^{17} levels are summarized in the level diagram of Fig. 13. The 531.4-keV line observed in both the singles and coincidence spectra could not be assigned to the possible 1.91→1.37-MeV branch (537.3 keV expected), since the two energies did not match, well outside the errors for each. Thus the 531.4-keV line was assigned to the known 3.67→3.13 transition.[53] The possibility of a weak 537.3-keV 1.91→1.37-MeV branch could not be excluded—hence the dotted line in the N^{17} energy-level scheme of Fig. 13.

The lifetime limits for the 1.37- and 1.91-MeV levels permit spins of $\leq\frac{3}{2}$ and $\geq\frac{5}{2}$ to be deduced for these levels, given $\frac{1}{2}$ for the N^{17} ground-state spin.[54] The spin of the F^{17} $T=\frac{3}{2}$ analog of the 1.37-MeV state has been determined as $\frac{3}{2}^+$,[55] in agreement with this work. A tentative spin assignment of $\frac{3}{2}$ has also been made on the basis of a $2J+1$ dependence of total cross-section data for Li+B reactions.[56]

[53] V. P. Hart, E. Norbeck, and R. R. Carlson, Phys. Rev. **137**, B17 (1965).
[54] M. G. Silbert and J. C. Hopkins, Phys. Rev. **134**, B16 (1964).
[55] J. R. Patterson, H. Winkler, and C. S. Zaidins, Phys. Rev. **163**, 1051 (1967).
[56] R. L. McGrath, Phys. Rev. **145**, 802 (1966).

L. O^{16}

The 8.87→6.13-MeV transition was observed in the Li^7+B^{11} spectra (Fig. 12). The shift analysis took into account the nature of the 1.7-MeV peak, which consisted of a predominant two-escape peak from the 2.74-MeV 8.87→6.13 branch plus a weaker 1.75-MeV peak from the 8.87→7.12-MeV branch. The expected shift of the unresolved doublet was determined using known branching ratios for the 8.87-MeV level[57] as well as relative efficiencies for the 1.75- full-energy and 2.74-MeV two-escape peaks. The resulting weighted-average lifetime, based on two measurements, was $\tau_m = (3.7\pm1.3)\times10^{-13}$ sec. This is in poor agreement with a reported result of $\tau_m = (1.92\pm0.29)\times10^{-13}$ sec.[58] The error in the present result is about equally due to the $\langle\cos\theta_{c.m.}\rangle$ uncertainty and to background subtraction errors. The transition energy (weighted average) was 2740.4±1.0 keV, in good agreement with a value of 2739±5 keV deduced from accurate excitation energies reported for O^{16} levels.[25]

M. O^{18}

Transitions were observed in the Li^7+C^{12} and C^{13} spectra. No significant lifetime information was obtained. Transition energies for decay from the O^{18} 1.98-, 3.55-, 3.63-, and 3.92-MeV levels were measured. The results (Table II) are in good agreement with, but more accurate than, values determined from compiled O^{18} excitation energies.[22]

N. F^{18}

Numerous F^{18} transitions were observed in the Li^6+O^{16} spectra (Fig. 6). The lifetime and branching-ratio results reported by the Brookhaven group[59,60] for levels in F^{18} were used to identify lines suitable for lifetime analysis. Since many F^{18} levels were fed extensively by branches from higher levels, most observed transitions were not suitable for analysis. In addition, the Q value for many of the low-lying levels of F^{18} was sufficiently large to permit large fractions of F^{18} recoil in vacuum. One transition found suitable for analysis was that from the F^{18} 4.36-MeV level. The resulting two-standard-deviation lifetime limit obtained was $<6.1\times10^{-13}$ sec, where the rather large limit is due to an estimated error for a small recoil fraction in vacuum. Possible spins of 0, 1, 2, and 3 have been delimited from angular-correlation work for the 4.36→3.06-MeV transition.[60] If the spin of the 4.36-MeV level were 0,

[57] D. H. Wilkinson, D. E. Alburger, and J. Lowe, Phys. Rev. **173**, 995 (1968).
[58] R. E. Pixley and W. Benenson, Nucl. Phys. **A91**, 177 (1967).
[59] E. K. Warburton, J. W. Olness, and A. R. Poletti, Phys. Rev. **155**, 1164 (1967).
[60] J. W. Olness and E. K. Warburton, Phys. Rev. **156**, 1145 (1967).

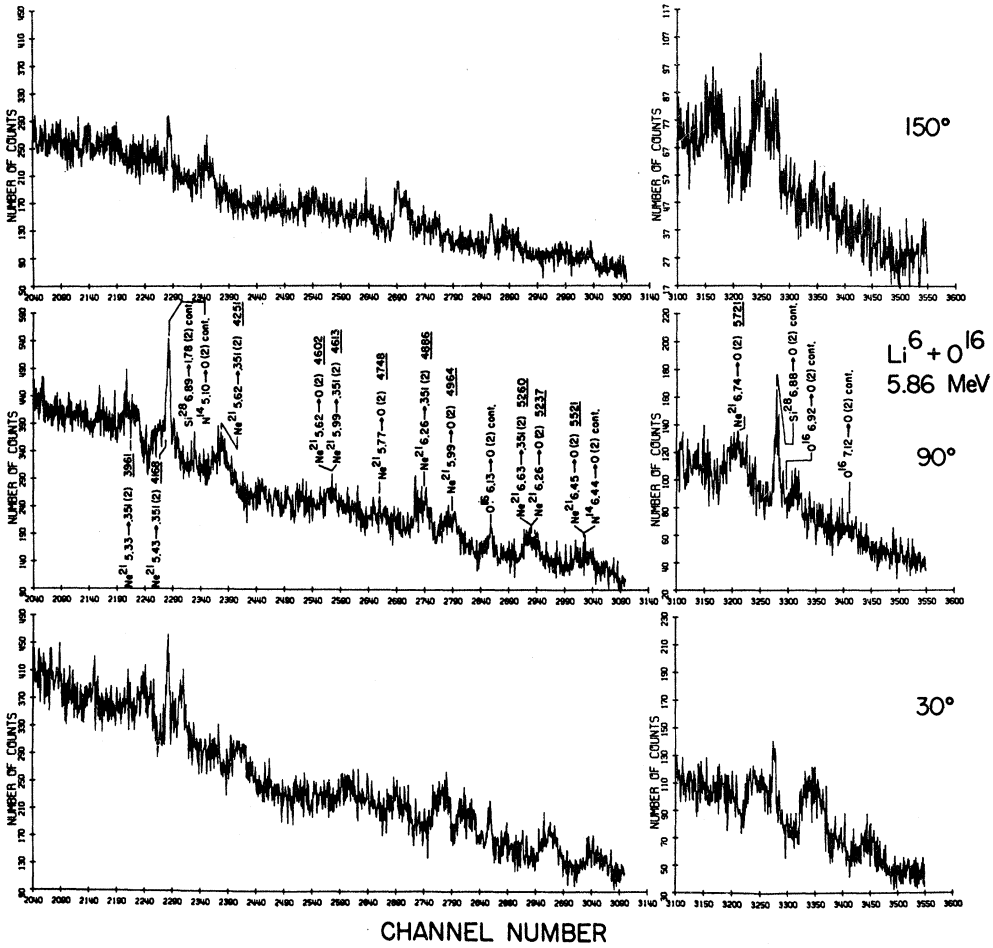

FIG. 14. Portion of the γ-ray spectra observed at $\theta_\gamma=30°$, 90°, and 150° in the 5.86-MeV Li^6 bombardment of a SiO target. The presentation is identical to that of Fig. 6.

the experimental limit would imply enhancements over the Weisskopf single-particle estimate of at least 125 for the $E2$ and 270 for the $M2$ transition to the 2^+ 3.06-MeV level. The $E2$ enhancement is greater than that permitted by the $\Gamma_\gamma \leq Z^2\Gamma_{\gamma W}$ sum rule.[61] The $M2$ enhancement is much greater than those observed for $A \leq 40$ nuclei.[62] Thus a spin assignment of 0 may be ruled out for the F^{18} 4.36-MeV level.

O. Ne^{20}

Transitions from the 1.63-MeV level were observed and analyzed for the Li^6+O^{16} and Li^7+O^{16} spectra. The 1.63-MeV-level measurements and results for the Li^6+O^{16} spectra were discussed in Sec. III. The resulting lifetime for the 1.63-MeV level, based on an error-weighted average over three shift and line-shape measurements, was $\tau_m=1.27\pm0.24$ psec. Previously reported lifetime measurements for the Ne^{20} 1632-keV state yield a weighted average of 0.95 ± 0.15 psec.[62] The most accurate of the previously reported measurements was 1.23 ± 0.12 psec.[63]

P. Ne^{21}

Transitions were observed in the Li^6+O^{16} spectra (Fig. 14). Numerous lines in the spectra above 5 MeV were identified as due to transitions in Ne^{21}, using compiled level energies[22] for Ne^{21} and noting that no other residual nucleus from the Li^6+O^{16} reaction was a possible source for lines >5 MeV in energy. The lines assigned to transitions in Ne^{21} were in all cases quite weak, so that the most reliable lifetime results were limits based on broadening measurements. For a broadening-attenuation factor of $F_B'>0.5$, the two-standard-deviation lifetime limit for the Ne^{21} 5.33-, 5.62-, 5.77-, 5.99-, 6.26-, and 6.74-MeV levels was $\tau_m<7\times10^{-13}$ sec. Since the Ne^{21} lines were quite weak,

[61] D. H. Wilkinson, in *Nuclear Spectroscopy*, edited by F. Ajzenberg-Selove (Academic Press Inc., New York, 1960), Pt. B, Chap. V.F.

[62] S. J. Skorka, J. Hertel, and T. W. Retz-Schmidt, Nucl. Data **2**, 347 (1966).

[63] H. C. Evans, M. A. Eswaran, H. E. Gove, A. E. Litherland, and C. Broude, Can. J. Phys. **43**, 82 (1965).

and no well-known internal calibration lines were present in the high-energy portion of the Li^6+O^{16} spectra, no attempt was made to measure transition energies.

V. SUMMARY

Error-weighted-average lifetime results for the present investigation have been summarized in Table II. Errors for the lifetime measurements summarized in Table II are one standard deviation error limits. In the case of a limiting value for a lifetime, the limit given in Table II is a two standard deviation limit. Comparison between the present results and previously reported measurements has been made in the appropriate subsections of Sec. IV.

An incidental result of this work was the determination with improved accuracy of a number of transition energies for nuclei produced in the reactions studied. The results are summarized in Table II. The results are in good agreement with, but more accurate than, transition energies determined from compiled excitation energies,[22] except for the case of B^{11} transitions, discussed in Sec. IV B.

ACKNOWLEDGMENTS

The author is indebted to Professor R. R. Carlson for his advice throughout the course of this work. Discussions concerning analysis and interpretation of the data with Professor R. T. Carpenter, Dr. S. I. Baker, and Dr. R. A. Mendelson, Jr., were of great value. Dr. W. A. Seale, L. Rice, B. Aldrich, and G. W. Hartnell rendered valuable assistance during long data runs.

PHYSICAL REVIEW VOLUME 179, NUMBER 4 20 MARCH 1969

Reaction $^{12}C(^3He, d)^{13}N$ and Stripping to Unbound States*

H. T. FORTUNE†

Department of Physics, Florida State University, Tallahassee, Florida 32306 and Argonne National Laboratory, Argonne, Illinois 60439

AND

T. J. GRAY,‡ W. TROST,§ AND N. R. FLETCHER

Department of Physics, Florida State University, Tallahassee, Florida 32306

(Received 13 November 1968)

Excitation functions of deuterons from the $^{12}C(^3He, d)^{13}N$ reaction over the bombarding-energy range 12–19 MeV were measured at several angles for the ground-state deuterons and at a laboratory angle of 40° for deuterons leading to the ground state, to the first excited state, and to the unresolved second and third excited states. Detailed angular distributions were measured at 16, 17, and 18 MeV for the ground state through the third excited state and at 19 MeV for the ground state through the seventh excited state. The ground-state angular distributions were analyzed with the conventional distorted-wave Born approximation. For the excited states, all of which are unstable with respect to proton decay, a number of alternative methods of calculation were attempted and the results were compared.

I. INTRODUCTION

IN a continuing study of ^{3}He-induced reactions in light nuclei,[1–3] the reaction $^{12}C(^3He, d)^{13}N$ has been studied over the bombarding energy range 12–19 MeV. In ^{13}N, only the ground state is stable against emission of a proton (Fig. 1), which is the captured particle in a $(^3He, d)$ reaction. There has been recent theoretical interest[4] in stripping to unbound states, with apparently some success in applying this theory.[5]

Wegner and Hall,[6] using 21.6- and 24.7-MeV ^{3}He particles, measured the angular distributions for the $^{12}C(^3He, d)^{13}N$ reaction, leading to the ground state, the first excited state, and the unresolved second and third excited states of ^{13}N. The data show little change for the 3-MeV change in bombarding energy. Their results were analyzed with the use of the plane-wave Born approximation (PWBA). They found that the

* Research supported in part by the Air Force Office of Scientific Research, Office of Aerospace Research, U.S. Air Force, under AFOSR Grant No. AFOSR-440-67, and the National Science Foundation (Grant No. NSF-GP-5114), and in part under the Auspices of the U.S. Atomic Energy Commission.

† NASA Fellow at the Florida State University. Present address: Argonne National Laboratory, Argonne, Ill.

‡ Present address: North Texas State University, Denton, Tex.

§ Present address: Physikalisches Insitut der Universität, Heidelberg, Germany.

[1] F. Dunnill, T. J. Gray, H. T. Fortune, and N. R. Fletcher, Nucl. Phys. A93, 201 (1967); N. R. Fletcher, J. D. Marshall, and R. H. Davis, *ibid.* 70, 471 (1965).

[2] H. T. Fortune, T. J. Gray, W. Trost, and N. R. Fletcher, Phys. Rev. 173, 1002 (1968).

[3] T. J. Gray, H. T. Fortune, W. Trost, and N. R. Fletcher (unpublished).

[4] R. Huby and J. R. Mines, Rev. Mod. Phys. 37, 406 (1965).

[5] J. L. Alty, L. L. Green, R. Huby, G. D. Jones, J. R. Mines, and J. F. Sharpey-Schafer, Phys. Letters 20, 664 (1966); Nucl. Phys. A97, 541 (1967).

[6] H. E. Wegner and W. S. Hall, Phys. Rev. 119, 1654 (1960).